AD-A145 183 AN INFRARED STUDY OF AMBIENT TEMPERATURE CHLOROALUMINATES AS A FUNCTION O..(U) STATE UNIV OF NEW YORK AT BUFFALO DEPT OF CHEMISTRY S TAIT ET AL. JUL 84 1/1

UNCLASSIFIED SUNYBUF-AC/TR-21-N00014-79-C-0682 F/G 20/6 NL

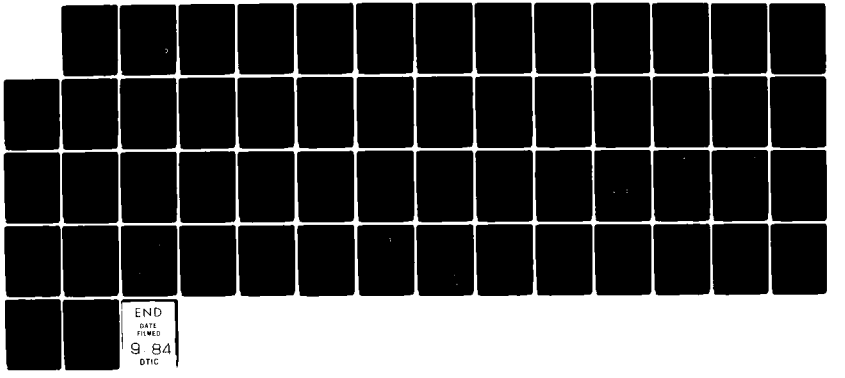

END
DATE FILMED
9 84
DTIC

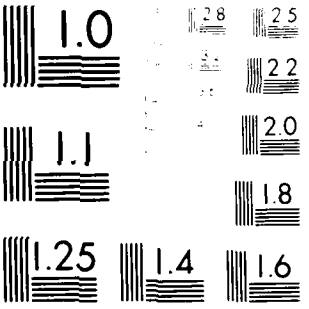
1.0
2.8
2.5
2.2
1.1
2.0
1.8
1.25
1.4
1.6

UNCLASSIFIED

(2)

SECURITY CLASSIFICATION OF THIS PAGE (When Data Entered)

REPORT DOCUMENTATION PAGE		READ INSTRUCTIONS BEFORE COMPLETING FORM
1 REPORT NUMBER SUNYBUF/DC/TR-21	2. GOVT ACCESSION NO.	3 RECIPIENT'S CATALOG NUMBER
4 TITLE (and Subtitle) An Infrared Study of Ambient Temperature Chloroaluminates as a Function of Melt Acidity		5 TYPE OF REPORT & PERIOD COVERED 6. PERFORMING ORG. REPORT NUMBER
7. AUTHOR(s) Stephen Tait and Robert A. Osteryoung		8 CONTRACT OR GRANT NUMBER(s) N00014-79-C-0682
9. PERFORMING ORGANIZATION NAME AND ADDRESS Department of Chemistry State University of New York at Buffalo		10 PROGRAM ELEMENT, PROJECT, TASK AREA & WORK UNIT NUMBERS NR-051-715
11 CONTROLLING OFFICE NAME AND ADDRESS Office of Naval Research Chemistry Program Arlington, VA 22217		12. REPORT DATE July, 1984 13 NUMBER OF PAGES 45
14 MONITORING AGENCY NAME & ADDRESS(if different from Controlling Office)		15. SECURITY CLASS. (of this report) Unclassified 15a DECLASSIFICATION DOWNGRADING SCHEDULE

16 DISTRIBUTION STATEMENT (of this Report)

Approved for Public Release: Distribution Unlimited

17. DISTRIBUTION STATEMENT (of the abstract entered in Block 20, if different from Report)

DTIC ELECTE SEP 5 1984 S D B

18 SUPPLEMENTARY NOTES

Prepared for Publication in Inorganic Chemistry

19. KEY WORDS (Continue on reverse side if necessary and identify by block number)

Infra-Red Studies; Molten Salts, Ionic Association

20. ABSTRACT (Continue on reverse side if necessary and identify by block number)

The infrared spectra of butyl pyridinium chloride/aluminum chloride and 1-methyl 3-ethyl imadazolium chloride/aluminum chloride room temperature molten salts have been examined over a range of mole ratios (acidities). Bands observed in the 4000-630 cm^{-1} range have been assigned and spectral changes attributed to the formation of ion pairs, which may involve distortion of the aromatic ring since there is an accompanying loss of aromatic character. This effect is more pronounced in the imidazolium melts where more highly basic melts can be studied

DD FORM 1 JAN 73 1473 EDITION OF 1 NOV 65 IS OBSOLETE

Unclassified

SECURITY CLASSIFICATION OF THIS PAGE (When Data Entered)

due to the greater liquidus range. Several isobestic points are reported.

Addition of H_2O/D_2O to imidazolium melts gave rise to distinct new features in the spectra. In an acidic melt a new spectrum emerged after spectral subtraction which is believed to be due to the formation of either AlO(OH) or, more likely, $AlOHCl_2$. Addition of H_2O/D_2O to a basic melt gave a complex spectrum.

OFFICE OF NAVAL RESEARCH

Contract N00014-79-C-0682

Task No. NR-051-715

TECHNICAL REPORT NO. 21

An Infrared Study of Ambient Temperature Chloroaluminates as a Function of Melt Acidity

by

Stephen Tait and Robert A. Osteryoung

Prepared for Publication

in

Inorganic Chemistry

Department of Chemistry
State University of New York at Buffalo
Buffalo, New York 14214

July, 1984

ABSTRACT

The infrared spectra of butyl pyridinium chloride/aluminum chloride and 1-methyl 3-ethyl imidazolium chloride/aluminum chloride room temperature molten salts have been examined over a range of mole ratios (acidities). Bands observed in the 4000-630 cm^{-1} range have been assigned and spectral changes attributed to the formation of ion pairs, which may involve distortion of the aromatic ring since there is an accompanying loss of aromatic character. This effect is more pronounced in the imidazolium melts where more highly basic melts can be studied due to the greater liquidus range. Several isobestic points are reported.

Addition of H_2O/D_2O to imidazolium melts gave rise to distinct new features in the spectra. In an acidic melt a new spectrum emerged after spectral subtraction which is believed to be due to the formation of either AlO(OH) or, more likely, $AlOHCl_2$. Addition of H_2O/D_2O to a basic melt gave a complex spectrum.

INTRODUCTION

Until recently it has been accepted that melt equilibria in N-(1-butyl)pyridinium chloride (BuPyCl)/aluminum chloride ($AlCl_3$) and the 1-methyl 3-ethyl imidazolium (ImCl)/aluminum chloride room temperature melts can be described by the two equilibria (1):

$$AlCl_3 + Cl^- \rightleftharpoons AlCl_4^-$$
$$AlCl_3 + AlCl_4^- \rightleftharpoons Al_2Cl_7^-$$

The former is dominant in basic melts i.e. where the $AlCl_3$:BuPyCl mole ratio is less than 1 and the latter in acid melts where the ratio is greater than 1. The role of the cation had been ignored until Wilkes et al (2) and Popov (3) undertook NMR studies of this molten salt system (2,3) and of a similar 1-methyl 3-ethyl imidazolium chloride (ImCl) system (2). Both provided good evidence of ionic interaction (particularly on the basic side) and Wilkes et al proposed several oligomers to explain the observed behavior.

This problem has not been studied by IR spectroscopy due to the highly corrosive nature of the melts, the lack of resistant, wide transmission windows and the inability to compensate for the large molten salt absorbances encountered even in short pathlength cells. The recent acquisition of an FTIR spectrometer and the development of a transmission cell with silicon windows (a configuration thought to possess severe disadvantages) (4,5) has minimized these problems.

In this work the mid IR spectra of both the BuPyCl and ImCl/$AlCl_3$ melts have been studied as a function of acidity in order to examine the nature of the ionic interaction more closely. Water has also

been added to the melt in an attempt to find out more about the "aging" process in melts and the initial results are reported.

EXPERIMENTAL

The experimental details below have been compiled in accordance with the criteria laid down by a sub-committee of the Coblenz society for the comparison of computerized infrared spectra (6).

Instrument Information

The spectrometer was manufactured by Nicolet, Model 7199 and was used in unmodified form exclusively for transmission spectroscopy. The detector was a nitrogen cooled mercury-cadmium-tellurium detector (range 400-5000 cm^{-1} - noise equivalent power of 2×10^{-10} $W/hz^{1/2}$). The detector element had an area of 1 mm^2. The source was a water-cooled Globar and the beam splitter was germanium on a potassium bromide substrate (range 400-4000 cm^{-1}).

Data Collection

A Happ-Genzel apodization function was applied to the double-sided interferogram. The collection parameters used to obtain spectra at a resolution of 1 cm^{-1} are shown in Table 1. The times quoted include mirror return and acceleration to constant velocity but not the pre-collection beam equilibration delay.

Data collection, spectral subtraction and plotting of spectra were automated using the macro programming system developed in this laboratory.

Sampling Data

The dynamic range of the ADC was 15 bits and the word length

was 20 bits. A system of gain-ranging was used in the collection program which changed the sensitivity away from the center burst of the interferogram to allow detection of small signals.

Spectral Manipulation

For clarity of presentation smoothing has sometimes been used in spite of the fundamental objection raised by Grasseli et al (6) that band degradation occurs when data collected on an FTIR are smoothed. Spectra were, however, checked to see that significant absorbance peaks were neither created nor removed by this operation. Values for peak frequency and absorbance were taken from unsmoothed data. An 11 point 2nd order Savitsky-Golay algorithm was used for smoothing. The absorbance values found after subtraction of the empty cell were corrected for movements of the baseline caused by the different refractivities of the filled and empty cell.

No attempt was made to automatically remove water vapor absorbances from spectra. The region near 1650 cm^{-1} containing the sharpest absorbances for this purpose was obscured by absorbances attributable to the melt and small changes in the background were large relative to the water absorbance near 3500 cm^{-1}. Since the instrument was kept in an area of controlled low humidity and was continuously purged with nitrogen this was not a significant problem. However carbon dioxide bands could have led to confusion the instrument was purged for 15 minutes before spectra were run.

Sampling Accessories

All sampling accessories were supplied by Harrick Scientific Corporation. The cell consisted of a stainless steel body with a

teflon insert (see Figure 1). The cell windows were 13 mm in diameter and 2 mm wide polished silicon discs and were separated by half-moon spacers of 0.05 mm thickness. The assembly was screwed down to align the cell windows with the entrance and exit to the teflon plugs. The molten salts flowed through these hollow threaded plugs without contacting the stainless steel.

When the windows were kept parallel by the use of two spacers, 5 separate lagged interferograms were observed due to reflection, which transformed to give fringes (Figure 2). The unwanted interferograms could be removed in an empty cell by generating a straight line across the sections of the interferogram where the fringes occurred; however, in the presence of melts this led to distortion of the sample spectrum.

When the windows were tilted with respect to each other by using only one spacer (see Figure 3), the lagged interferograms disappeared and a flat baseline resulted on transformation (see Figure 2). The cell was maintained in this configuration for all samples; the procedure adopted for filling and emptying the cell is detailed below. The nominal cell pathlength was 0.025 mm and the cell volume was 6.3 µl. The pathlength of the cell was checked with the windows parallel using two spacers by measuring the frequency difference between fringes and the cell pathlength was found to be accurate to $\pm$5%.

The cell was filled using a 1 ml tuberculin syringe in a Vacuum Atmospheres Drybox maintained at <5 ppm oxygen and water by a Vacuum Atmospheres HE193/2 Dritrain purification system which circulated the box atmosphere through molecular sieves and a copper catalyst

bed to remove oxygen. The cell was angled to avoid trapping bubbles between the opaque silicon windows during filling and sealed with teflon stoppers. The cell was emptied without diassembly by slowly flushing with 5 ml of methylene chloride to remove the molten salt, 10 ml of methanol to dissolve any residual films and finally with 5 ml methylene chloride to remove the methanol. The cell was then flushed with argon and dried in vacuo for at least 20 minutes before being refilled with the next sample.

Chemicals

Anhydrous aluminum chloride (Fluka AG) was distilled once under vacuum in a sealed Pyrex tube from a mixture containing sodium chloride and aluminum wires. This procedure and the preparation of butyl pyridinium chloride (BuPyCl) has been described elsewhere (7).

Preparation of 1-methyl, 3-ethyl imidazolium chloride (ImCl) was based on a method described by Wilkes et al (8) using a pressure bottle assembly manufactured in our workshop. Following the reaction, a white precipitate formed on cooling and the residual ethyl chloride was vented. Since the product was highly hygroscopic (recrystallization on the open bench result in the formation of oils) it was dissolved in hot acetonitrile in a closed glassware apparatus and recrystallized by the addition of cooled ethyl acetate. Seeding assisted recrystallization. After two recrystallizations the product (mp 82-86°C) was filtered, dried under vacuum at room temperature and transferred to the drybox for storage.

RESULTS AND DISCUSSION

In previous studies (9) polyethylene had been used as the cell window material for IR work on similar molten salts because of its low background absorbance and inertness to the melt; however it does absorb strongly in the C-H stretching region (2800-3000 cm^{-1}) and its flexibility makes a fixed pathlength cell more difficult to obtain. Silicon windows were selected for this work as they appeared to be resistant to corrosion by melts of any acidity, could be arranged to give a reproducible cell pathlength and provided a wider transmission window.

The disadvantage of using silicon is its high refractive index which leads to high background absorbances ($\sim$0.75 abs units). In addition the spectrum of silicon (607-602 and 626-612 cm^{-1}) and of its impurities (carbon 607-602 cm^{-1} and oxygen 1125-1090 cm^{-1}) also interfere (10); however, since the melt does not interact with the windows, all but the major silicon absorbance at 620 cm^{-1} (i.e., absorbances less than 2 abs units) can be subtracted without any alteration to the sample spectrum. Where the absorbance exceeds 2 abs units (i.e. less than 1% transmission) subtraction becomes less accurate and the result is a confused differential. This work has, therefore, been restricted to the 4000-630 cm^{-1} range.

Melt spectra were recorded over a range of acidity from 0.8:1 to 2:1 $AlCl_3$/BuPyCl and 0.4:1 to 1.75:1 $AlCl_3$/ImCl. In order to compare melts of different acidity the spectra were corrected for cation dilution by multiplying the spectra by a correction factor after the background

cell window spectrum had been subtracted. The molar cation concentration is given by:

$$[R^+] = \frac{\text{Mole fraction}_{RCl} \cdot \text{Density} \times 10^3}{\text{Binary Molecular Weight}}$$

where R^+ = butyl pyridinium or imidazolium cation and the binary molecular weight is given by:

$$\text{Binary Molecular Wt.} = [(\text{Mole fraction}_{AlCl_3} * \text{Mol. Wt.}_{AlCl_3}) + (\text{Mole fraction}_{RCl} * \text{Mol. Wt.}_{RCl})]$$

The correction factor is the ratio of the cation concentration in a particular melt to the cation concentration in a 0.8:1 $AlCl_3$/BuPyCl for BuPyCl melts or in a 0.4:1 $AlCl_3$/ImCl for ImCl melts (see Table 2) (11). Thus, any absorbances unaltered by changes in melt acidity after correction are inferred to be due to vibrations which are not affected by melt interactions.

IR Spectra of $AlCl_3$/BuPyCl Melts

The IR spectrum of an empty cell alone and filled with 0.8:1 $AlCl_3$/BuPyCl melt are shown in Figure 4. The subtraction of these two spectra and a similar subtraction for a 1.8:1 $AlCl_3$/BuPyCl melt are shown in Figure 5. The peak frequencies and absorbances of the two melts are detailed in Table 3 and compared with the same data for the methyl pyridinium cation (12).

As expected there are both similarities and differences, most of the latter attributable to the presence of the butyl group. There is increased aliphatic C-H stretching (2850-3000 cm^{-1}), C-H/C-N mixed out of plane bending modes (1347-1454 cm^{-1}), C-N stretching (1251 cm^{-1}), aromatic C-H in plane bending (950-1230 cm^{-1}) and C-H bending at

686 cm^{-1}. The last band only occurs strongly where there are at least 4 adjacent methylene groups in the alkyl chain (13).

The spectra of acidic and basic melts were very similar. Many of the bands were sharp in the acidic melt but broader in the basic melt (e.g., 1214, 1320, 1464-1501, 1584 and 1634 cm^{-1}) and peak frequencies were lower by between 2-6 cm^{-1}. Both the loss of symmetry suggested by the first effect and the peak shift are indicative of an interaction, perhaps ion pair formation, though the magnitude suggests that this is not a strong effect. Similar, and more pronounced effects are observed in the ImCl-$AlCl_3$ melts (see below) where studies could be performed in more basic melts.

The absorbance change in intensity (9) at 1450-1500 cm^{-1} in acidic melts found by Gale and Osteryoung was observed but the bands at 1256 and 1360 cm^{-1} could not be reproduced. This may indicate that polyethylene windows employed in this earlier study were not inert to attack by acidic melts.

The main difference between acidic and basic melts was in the C-H stretching region. A new broad band emerged at 3018 cm^{-1} as the melt was made basic (see Figure 6). A similar band appears in the ImCl melts (see below), but the source of this band is not known.

In spite of the interference caused by this effect it appears that the intensities in the aliphatic C-H stretching region at 2970-2870 cm^{-1} are enhanced and that the intensities of C-H aromatic bands at 3130-3070 cm^{-1} are diminished as the acidity decreases. These changes indicate a loss in ring aromaticity, which has also been observed by NMR where proton chemical shifts tend toward those expected of a conjugated alkene as melts are made more basic (2,14).

Further differences arise in the 660-840 cm^{-1} region (see Figure 7). A multipeaked band was observed at 773 cm^{-1} in a 1.2:1 $AlCl_3$/BuPyCl melt with a shoulder at 782 cm^{-1}. The area of the band decreased with increasing acidity or basicity from a neutral melt (spectra could not be obtained in the neutral region itself as the melt solidified at room temperature). The band shape also distinctly altered and the peak altered to 772 cm^{-1} in 0.8:1 $AlCl_3$/BuPyCl and 768 cm^{-1} in 2:1 $AlCl_3$/BuPyCl melt. The shoulder at 782 cm^{-1} remained unaltered.

A large off-scale absorbance at 670-695 cm^{-1} varied in intensity in the same way but was only on-scale in the 2:1 $AlCl_3$/BuPyCl melt. The band consisted of a broad absorbance at 691 cm^{-1} with two peaks superimposed on it at 686 and 683 cm^{-1}. The absorption bands in this region were, however, very large.

The vibrational modes of pyridine assigned by Spinner (12) were based on the degenerate vibrational modes of benzene described by Lord et al (15). The aromatic out of plane modes are assigned to the 772 cm^{-1} and 683 cm^{-1} bands.

Association by the cation with species above or below the plane of the molecule (i.e., ion pairing) might reduce the intensity of the vibration. The 683 cm^{-1} band is more affected than the 772 cm^{-1} band. This postulated association is consistent with the observation of Wilkes et. al. (2) in NMR studies on these molten salts.

In summary, the change in band shape and intensity as the melt acidity is varied across the range suggest that intermolecular interaction, perhaps ion pair formation, is taking place in both the acidic and basic melts. Loss of aromaticity in the basic melts suggest that there may be some ring distortion associated with this interaction.

IR Spectra of $AlCl_3$/ImCl Melts

Infrared spectra for the 0.4:1 $AlCl_3$/ImCl and 1.5:1 $AlCl_3$/ImCl melts with silicon cell window absorbance subtracted are shown in Figure 8. The peak frequencies and absorbances for these two melts and for ImCl in methylene chloride are tabulated and assigned in Table 4. The same data for liquid imidazole is also included to differentiate bands which could be attributable to either the organic cation or inorganic species. The spectra have all been corrected for changes in cation concentration as before (see Table 2).

Imidazole has been the subject of several IR studies (16,17) and the spectrum is complicated by coupled vibrations arising from the heterocyclic ring and by considerable N-H..N association effects. In addition the position of bands is known to move when the ring positions are substituted (18) though 1,3 substitution removes N-H association.

In general, many of the bands found in the melt are in a similar position to those found in imidazole, but shifted to lower frequencies due to the inductive effect of the alkyl groups. Bands have been assigned on the basis of peak position, intensity and sensitivity to ring substitution relative to imidazole and its derivatives (19). The spectrum of ImCl in methylene chloride is very similar to that of

tne 0.4:1 $AlCl_3$/ImCl basis melt but is different in acidic melts, which suggests interaction, perhaps the formation of ion pairs, in both methylene chloride and the basic melt. The broadening and shift of peaks observed in the BuPyCl melts occurred more strongly in the ImCl melts; the change in peak frequency and absorbance of the most sensitive bands are tabulated in Table 5. The changes in the basic melts were more marked than for BuPyCl since more basic melts are attainable, but there were only small alterations to tne spectra over the acidic range. Thus specific interactions, perhaps ion pair formation, appear to be much stronger in the basic than in tne acidic melt.

Differences between tne acid and basic melts can be split into tnree regions 3600-1600, 1600-900 and 900-630 cm^{-1}.

3600-1600 cm^{-1}

Virtually no change was observed as the melt acidity was altered from 2:1 to 1:1 $AlCl_3$/ImCl and the resulting spectra were almost superimposable after correction for concentration changes (see Figure 9); thus Beer's law was obeyed for these melts down to at least 1% transmission, a fact which is most important in considering the changes taking place in tne basic melts.

In tne basic region there were considerable changes as the melt acidity was varied from 0.4:1 to 1:1 $AlCl_3$/ImCl (see Figure 10). A broad band with peaks at 3052 and 3018 cm^{-1} increased as the melt was made more basic and distorted the other bands in this region. The aromatic band at 3167 cm^{-1} diminished considerably and the band at 3114 cm^{-1} nearly disappeared under the 3052/3018 cm^{-1} band. An isosbestic point occurs at 3103 cm^{-1} indicating an interaction involving at least two

species whose concentrations vary with acidity. The aliphatic C-H stretching band at 2993 cm^{-1} shifts to 2982 cm^{-1} and the bands at 2963 and 2943 cm^{-1} behaved similarly becoming indistinguishable from the broad bands at 3052/3018 cm^{-1} in very basic melts.

As with the BuPyCl melt, the broad band at 3052/3018 cm^{-1} varies with melt acidity in the basic region. Bands in a similar region have been studied in liquid imidazole by Bellocq et al (16) who attributed them to a hydrogen bond, HN--H association. They deuterated imidazole in the 1 position and shifted the part of this region responsible for this effect. The band position (assuming a value of ν_{N-H}/ν_{N-D} of 1.34), shape and intensity is similar to that seen in this melt. While recent studies support Bellocq's et al explanation of the breadth and complexity of the bands in this region observed in imidazole (19,20) the presence of the band in the ImCl melt, however, should not be due to similar interaction, since both of the nitrogen atoms are substituted, but there is no obvious source of available proton, except for perhaps traces of water, in the melt. This band could possibly be due to a hydrogen bond type of interaction between Cl^- and H on C-2 of the imidazole ring. (Note that a band in a similar region varies with acidity in the BuPyCl melt.) In acid melts this broad band is absent and in the basic melts its intensity is clearly a direct function of the chloride concentration. Since this band also occurs in the basic BuPyCl melts it is not a function of the imidazole ring but could be related to an aromatic ring nitrogen or, as mentioned above, to a hydrogen bond between chloride and hydrogen in the butylpyridinium or imidazolium cation.

A broad low intensity absorbance in the 2600-2900 cm^{-1} region in the neutral and acidic melts becomes enlarged in the basic region and peaks emerged at 2866,2833(shoulder),2750 and at 2677 cm^{-1}.

In the 2600-1600 cm^{-1} region the absorbances are small and have been assigned previously to non-fundamental modes, i.e. overtones or combination bands (19). The absorbance found at 1765 cm^{-1} in 0.4:1 $AlCl_3$/ImCl is absent in acidic melts. The band at 1660-1680 cm^{-1}, which is observed in the 1.5:1 $AlCl_3$/ImCl melt but obscured in the 0.4:1 $AlCl_3$/ImCl melt is probably due to either an overtone of the 834 cm^{-1} band and/or combination of the 1033 and 645 cm^{-1} bands.

1600-900 cm^{-1}

In addition to the general broadening and shifting of peaks already mentioned a shoulder on the 1570 cm^{-1} peak emerges at 1590 cm^{-1} (see Figure 11). This enlarges to a separate peak at 1595 cm^{-1} in acidic melts and cannot be attributed to a combination band. The change in peak frequency and intensity is shown in Table 5.

Similar effects have been recognized in studies of $\alpha\beta$-unsaturated tertiary amines (21,22), where increases of peak frequency of 20-50 cm^{-1} have been observed in going from an $\alpha\beta$-unsaturated amine (enamine) to its perchlorate salt corresponding to the transformation:

$$\rangle C{=}C\text{-}N \rightarrow \rangle CH\text{-}C{=}N^{+}$$

For instance, 1-n-butyl-2-methyl-tetrahydropyridine absorbs at 1649 cm^{-1} in the base form and 1684 cm^{-1} as the perchlorate salt. For

aromatic rings this structural change amounts to a loss of aromaticity and cnaracteristics more similar to a conjugated tertiary amine. In the melts the shift between the acidic melt and the 1570 cm^{-1} peak is 25 cm^{-1}; thus it appears that the I or III forms of the cation (see Scheme 1) have more significance as the chloride concentration is increased.

900-630 cm^{-1} (Figure 12)

As for the BuPyCl melts the ring bending modes of vibration are the most sensitive to changes in melt acidity. The in plane ring bending band at 834 cm^{-1} diminishes with little change in peak frequency as the acidity is reduced and is replaced by a very broad band (794-899 cm^{-1}) in highly basic melts. Isosbestic points are observed at 823 and 853 cm^{-1} as this change takes place. Subtraction in this region is less accurate than in higher wave number regions.

The out of plane bending mode at 760 cm^{-1} shifts to higher frequencies and broadens significantly (see Table 5). The two modes of vibration are shown below (19) and it again appears that modes of vibration which distort the position of the ring nitrogen atoms are more sensitive to acidity changes. When this observation is linked

In plane ring bending

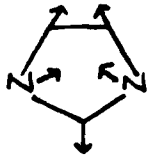

834 cm-1

Out of plane C-H bending

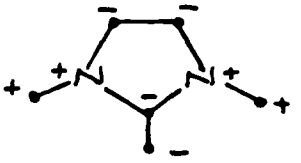

760 cm-1

with the enamine effect, the loss of aromaticity and the electronic repulsion between the chloride ion and the π electrons of the ring, distortion of the ring is suggested. This is illustrated in Scheme 1.

Wilkes et al (2) have suggested on the basis of their nmr studies that ion interactions occur in the form of oligomeric chains held together by ion-ion interactions in the basic melts. Two chlorides or one chloride and one tetrachloroaluminate or two tetrachloroaluminates, presumably with one above and below the plane of the ring are postulated as species. Popov has postulated the existence of ion pairs in the BuPyCl-$AlCl_3$ melt, also on the basis of nmr work (3). The results presented above, particularly with regard to the isosbestic point appearance and variation with acidity, appear to lend support to a two-species - i.e., ion pair - interaction. It is possible that whatever specific interaction takes place giving rise to the isosbestic point(s) depends only on whether or not the closest neighbor to the imidazolium ring is a single chloride ion; the formation of an oligomer by some time averaged proximity of a second chloride to the initial $BuPy^+/Im^+Cl^-$ "ion pair" may not result in additional perturbations sufficient to result in further IR spectral changes.

The frequency at 703 cm^{-1} could not be assigned to a cation vibration (unless it is the aliphatic C-H bending mode, which is unlikely (13)) and it increased in size without any change in peak frequency as the melt acidity was increased. Since Al-O stretching bands are known to exist in this region (23,24), the possibility that this was linked to the "aging" of melts was examined by adding water.

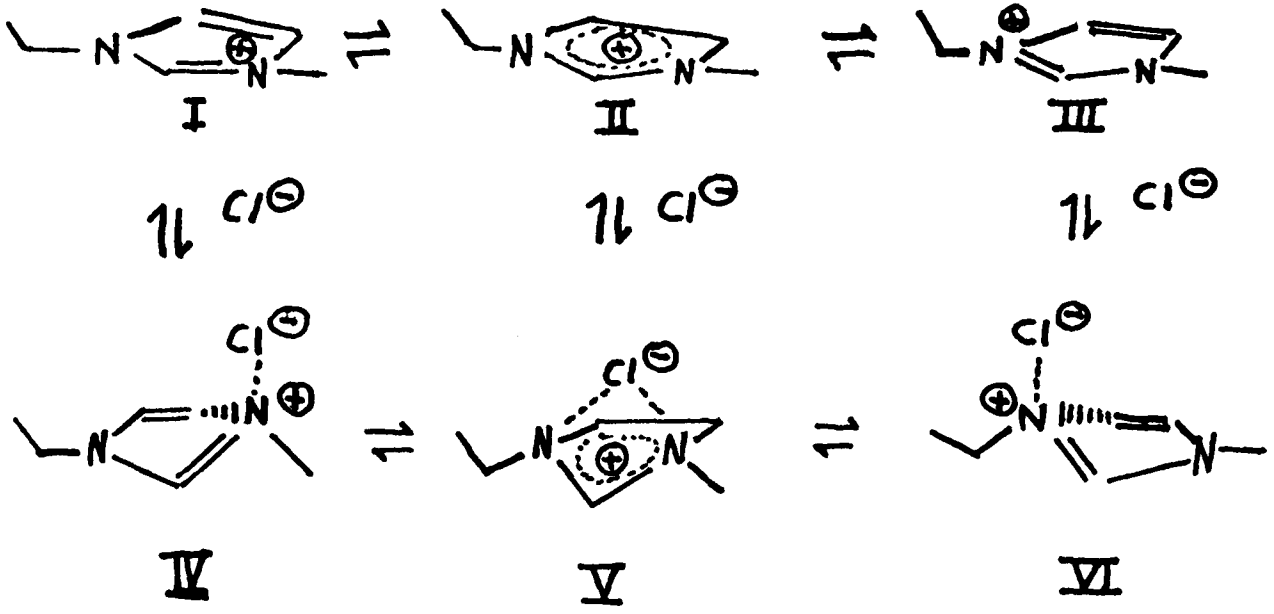
I
II
III
Cl⊖
Cl⊖
Cl⊖
IV
V
VI

Addition of Water to $ImCl/AlCl_3$ Melts

1.6:1 $AlCl_3/ImCl$ Acid Melt

Acidic melts react with water in a highly exothermic manner with the evolution of hydrogen chloride and the formation of a white precipitate. This redissolves on stirring and the spectrum of this melt (20 mM water) after subtraction of a reference 1.6:1 $AlCl_3/ImCl$ melt spectrum is shown in Figure 13. The same spectrum for the addition of D_2O is shown in Figure 14. The peak frequencies are compared in Table 6 with other aluminoxy species.

The subtracted spectrum only contains three bands at 3323, 1119 and 703 cm^{-1}, which increase linearly in magnitude with further additions of water. Both the 3323 and 1119 cm^{-1} bands disappeared when D_2O was added (60 mM) (apart from some traces of water in the D_2O) and new bands were found at 2477 and 853 cm^{-1}. The ratio of the two bands in each case was close to the theoretical shift of 0.76 and the bands were assigned to O-H stretching and O-H bending respectively. These bends are typical for an inorganic compound containing a hydroxy group (23). The 703 cm^{-1} band shifts by only a factor of 0.94 and was assigned to an Al-O-H stretching mode. A similar band is found in the spectra of aluminum oxide, aluminum hydroxide (see Table 6) and chloroaluminoxy species (24-26) though studies on the latter were obtained in aqueous media where the coordination of water and the formation of dimers complicate the spectrum. The absence of any Al-O-Al absorbances which typically occur near 2400 cm^{-1} (e.g., as in aluminum oxide) indicate that dimers are not formed in the acidic melt (25). Since the spectrum shows

no dimers the initially insoluble material must be dissolving up as a monomeric species such as AlO(OH), $Al(OH)Cl_2$ or $Al(OH)_2Cl$.

A study by Moolenaar et al (24) showed that a dihydroxy anion $AlO(OH)_2^-$ has absorbances at 900, 705 and 540 cm^{-1}. By analogy $Al(OH)_2Cl$ becomes unlikely as only one of the two possible bands visible in the transmission range is observed. Differentiating between AlO(OH) and $Al(OH)Cl_2$ is difficult as the IR region below 600 cm^{-1} is obscured by melt and window absorbances which prevent a search for the presence of Al-Cl stretching or dihydroxy antisymmetric bending modes. Of the two species the $AlOHCl_2$ is the more probable as the hydrogen atom on AlO(OH) would be shared leading to shifted peak frequencies and broader bands. In addition, previous electrochemical studies (1,27) suggested that AlOCl was the aluminoxy species arising in acid melt when oxide was added and $Al(OH)Cl_2$ is closer to this than AlO(OH).

Further additions of water to the melt led to the emergence of other bands in the spectrum (a broad multi-peaked band centered at 2175 cm^{-1} and another at 1230 cm^{-1}) possibly indicating the presence of other species at higher concentrations of added water.

Addition of Water to a 0.4:1 $AlCl_3$/ImCl Melt

Water (60 mM) reacted slowly with the basic melt to give a white precipitate which redissolved on stirring. (Not all of this precipitate redissolved when water was added to an approximately neutral melt.) The IR spectrum of the melt and redissolved precipitate after subtraction of a reference 0.4:1 $AlCl_3$/ImCl melt was complex, but showed similarities with spectra obtained by Riesgraf and May (26), who added freshly

prepared aluminum hydroxide gels to aluminum chloride solutions. At least three bands were observed in the O-H stretching region (3520(?), 3350, 3100 cm^{-1}) and two in the O-H bending region (1180, 1190 cm^{-1}). The remaining bands in the spectrum are weak and/or broad, though similarities exist between this spectrum and that of Riesgraf and May (26). On addition of D_2O (60 mM) the bands assigned to the hydroxyl group all shifted to lower frequencies by a factor close to 0.76 as before.

Recent work suggested that water reacts to form HCl and some unknown aluminum hydroxy species (28).

The formation of an Al-OH species in the chloroaluminate melt explains some of the results obtained during an electrochemical study of oxide and water addition in a basic BuPyCl/$AlCl_3$ melt in the presence of Ti(IV) (1). Two Ti(IV) reduction waves were found which varied with oxide concentration as a result of the equilibria:

$$O^{=} + AlCl_4^{-} \rightleftarrows AlOCl_2^{-} + 2Cl^{-}$$

$$TiCl_6^{=} + AlOCl_2^{-} \rightleftarrows TiOCl_4^{=} + AlCl_4^{-}$$

the latter equilibrium being quite slow. The addition of water shifted the Ti(IV) equilibrium to the left, indicating that water acted to remove $AlOCl_2^{-}$. The formation of an Al-OH-Cl species would account for the observed chemistry.

Table 1

Spectrometer Settings for Data Collection at 1 cm^{-1} Resolution

Data collection	
# of data points / interferogram	16384
# of transform points	32768
# of data points berore centre burst	256
High pass filter (hz) equivalent to a cut-off at 85cm-1	100*
Low pass filter (Khz) equivalent to a cut-off at 8530cm-1	10*
Scanning measurements	
# of scans	1000
Pre-collection beam delay (secs)	5
Total measurement time (secs)	1561
Scanning time (secs)	885
Mirror velocity (mms retardation/sec)	11.72
Retardation between points (mms)	6.86E-4

* This is the nominal roll-off frequency (3dB down point) of a Butterworth high/low pass noise filter

Table 2

IMIDAZOLIUM CHLORIDE/ALUMINUM CHLORIDE MELTS

Cation Concentration Correction Factors for the Normalization of BuPyCl and ImCl Melt Spectra

Mole Ratio ($AlCl_3$/ImCl)	Melt Density[1] (gm/cc)	Mole Fraction ImCl	Binary Melt Molecular Wt.	Cation Conc'n (Moles/litre)	Correction Factor
0.4	1.21	0.71	142.8	6.02	1.0
0.55	1.23	0.65	142.0	5.63	1.07
0.7	1.25	0.59	141.1	5.22	1.15
0.85	1.27	0.54	140.5	4.88	1.23
0.95	1.28	0.51	140.1	4.66	1.29
1.0	1.28	0.50	140.0	4.57	1.32
1.25	1.31	0.44	139.2	4.22	1.43
1.5	1.34	0.40	138.7	3.87	1.56
1.75	1.35	0.36	138.1	3.52	1.71
2.0	1.38	0.33	137.7	3.31	1.82

BUTYL PYRIDINIUM CHLORIDE/ALUMINUM CHLORIDE MELTS

Mole Ratio $AlCl_3$/BPC	Melt Density (gm/cc)	Mole Fraction BuPyCl	Binary Melt Molecular Wt.	Cation Conc'n (Moles/litre)	Correction Factor
0.8	1.22	0.56	154.8	4.41	1.0
0.85	1.23	0.54	154.0	4.31	1.02
0.9	1.23	0.53	153.6	4.24	1.04
0.95	1.24	0.51	153.0	4.13	1.07
1.25	1.28	0.44	150.2	3.75	1.17
1.5	1.30	0.40	148.7	3.50	1.26
1.75	1.32	0.36	147.1	3.23	1.36
2.0	1.33	0.33	146.0	3.00	1.47

1. Extrapolated or interpolated from data by Wilkes et al (11).

TABLE 3

Band Assignment	Methyl pyridinium iodide crystal		0.8:1 $AlCl_3$/BuPyCl Melt		1.8:1 $AlCl_3$/BuPyCl Melt	
	Peak Freq	Abs	Peak Freq	Abs [1]	Peak Freq	Abs [1]
	3134	0.1	3134	0.41	3132	0.27
	3118	0.1	3121	0.32		
Ar C-H str	3081	0.05	3090	0.58	3091	0.47
Ar C-H str/be	3074	0.25	3078	0.54		
	3056	0.1	3054	0.43	3048	0.08
Ar C-H str as	3038	0.45				
N-H str ass'n			3018	0.31		
Me C-H str as	2990	0.15				
Me C-H str sym	2967	0.05	2967	1.15	2968	0.81
Aliph C-H str			2940	0.91	2938	0.57
"			2906	0.52		
"			2878	0.78	2879	0.49
"			2870	0.64	2870	0.30
Arom C-C str	1632	0.8	1634	0.87	1634	1.01
"	1581	0.15	1583	0.22	1584	0.16
Arom str/def	1501	0.8	1501	0.70	1501	0.78
"	1486	0.9	1488	1.14	1489	1.42
Comb 681/783			1464	0.70	1466	0.60
Me C-H as be	1444	0.1	1444	0.38		
Me C-H as be	1419	0.05				
			1384	0.33	1384	0.21
Me C-H sym be	1347	0.01	1350	0.25	1352	0.14
Ring be i/p sym	1318	0.03	1320	0.38	1320	0.24
"	1287	0.3	1285	0.30	1285	0.14
"	1224	0.15	1251	0.24	1251	0.10
"	1210	0.3	1214	0.35	1214	0.18
Ring be i/p as	1189	0.7	1175	0.77	1176	0.89
	1150	0.15				
C-H be i/p	1135	0.25	1118	0.23	1118	0.20
C-H be i/p	1057	0.20	1064	0.24	1064	0.17
I/p str as	1025	0.1	1029	0.18	1029	0.09
Ring be o/p	954	0.1	955	0.20	956	0.18
Ring be o/p as	868	0.05				
Ring be i/p as	800	0.02			818	0.16
Me C-H be ?			783	0.55	781	0.55
Ring be o/p as	773	0.70	772	1.14	768	1.31
"	771	0.79				
			738	0.21	735	0.24
Ring be o/p sym	678	0.9				
CH_2 be			686	4.0	681-686	4.0

Abbreviations

str - stretching
be - bending
def - deformation
i/p - in-plane
o/p - out of plane
sym - symmetrical
as - asymmetrical
ass'n - association

1. Absorbance values have been corrected for non-zero baseline error arising out of the difference in refractive index of the cell empty and filled with melt.

Comparison of the IR spectra of 0.8:1 and 1.8:1 $AlCl_3$/BuPyCl melts with the methyl pyridinium iodide

TABLE 4

Band Assignment	0.4:1 $AlCl_3$/ImCl M		1.5:1 $AlCl_3$/ImCl Melt		0.5M ImCl in CH_2Cl_2		Imidazole[19]
	Peak Freq	Abs	Peak Freq	Abs	Peak Freq	Abs	Peak Freq
Arom C-H str	3148	0.57	3167	1.0	3145	0.1	
"			3122	0.87			3124
			310	0.73			3105
N-H/O-H ass'n					3074	0.18	
"	3052	1.22			3039	0.30	3021
"	3018	1.20					
Aliph C-H str			2993	0.36	2999	0.25	
"	2982	1.38	2963	0.25			
"			2943	0.20	2956	0.42	
N-H ?	2866	0.48			2865	0.14	
HCl ?	2833	0.28					
N-H ?	2749	0.09			2730	0.04	2800
HCl ?	2677	0.02					2587
N-H ass'n	1764	0.13			1732	0.05	
Comb			1678	0.10			
C-C=N$^+$-			1594	0.90			
Comb					1587	0.09	1573
Ring str sym	1569	1.22	1569	1.42	1573	0.22	1541
"	1464	0.60	1469	0.80	1467	0.11	1490
"	1458	0.60	1454	0.68	1454	0.09	1450
Me C-H be as	1427	0.38	1428	0.51	1428	0.08	
"	1389	0.35	1390	0.39	1388	0.08	
Ring str sym	1355	0.32	1357	0.39	1355	0.07	1323
Me C-H be sym	1344	0.32	1344	0.41	1343	0.09	
Ring str sym	1336	0.44	1336	0.42	1337	0.09	
Ring C-H be sym	1302	0.20	1292	0.13	1302		1260
N-H i/p be	1252	0.17	1246	0.16			1242
Ring str sym	1179	1.50	1167	2.54	1178	0.37	1140
Ring C-H i/p be	1108	0.22	1108	0.50			1099
Ring C-H i/p be	1080	0.31	1090	0.35			1052
Comb							972
Comb	1027-1033	0.17			1037	0.07	
N-H i/p be /C-H i/p be	959	0.16	959	0.14	959	0.02	934
Ring i/p be					896	0.08	894
C-H i/p be			834	1.13			835,827
	794-899	0.29					
Ring o/p be as							756,736
"	761	0.35	749	1.22	750	*	
Al-O str	704	0.09	703	0.3		*	
Ring be as	651	0.53	645	0.85	650	*	657
Ring be as	617-631	> 8.0 **	618-630	> 8.0 **		*	619

sym - symmetric as - asymmetric i/p - in plane o/p - out of plane str - stretching be - bending
* - obscured by C-Cl stretching absorbance ** combined with SI cell window absorbance

Comparison of the IR spectra of 0.4:1 and 1.5:1 $AlCl_3$/ImCl melts, 0.5M IC in methylene chloride and liquid imidazole

Table 5

Comparison of Peak Frequency and Intensity Changes Occurring with Melt Acidity

Mole Ratio $AlCl_3$/	Arom C-H stretch		Aliph C-H stretch		-C=N- stretch		Ring stretch		Ring i/p bending		Ring o/p bending	
	Peak Freq.	Abs	Peak Freq.	Abs	Peak Freq.	Abs	Peak Freq.	Abs	Peak Freq.	Abs	Peak Freq	Abs
0.40:1	3148	0.63	2981	1.43	1590	0.29	1178	1.48	834	0.34	760	0.46
0.55:1	3154	0.73	2983	1.25	1590	0.38	1175	1.44	838	0.45	758	0.60
0.70:1	3156	0.85	2985	1.05	1591	0.48	1172	1.55	837	0.58	754	0.84
0.85:1	3157	0.90	2987	0.76	1592	0.64	1170	1.98	837	0.76	751	1.04
0.95:1	3158	1.08	2988	0.52	1592	0.67	1168	1.57	837	0.95	747	1.05
1.0:1	3159	1.02	2990	0.40	1595	0.72	1170	1.87	838	1.19	747	1.20
1.20:1	3159	0.98	2991	0.40	1595	0.71	1169	2.15	837	1.09	747	1.30
1.50:1	3161	1.00	2992	0.39	1595	0.78	1169	2.14	836	0.98	747	1.42
1.75:1	3161	1.03	2993	0.40	1595	0.85	1169	2.46	835	1.08	747	1.62
Peak shift between 0.4:1 and 1.0:1 melts	-11		-9		5		8		4		13	
Peak shift between 2.0:1 and 1.0:1 melts	2		3		0		1		3		0	

Table 6

Comparison of the IR Peak Frequencies of Aluminoxy Species

Compound	Peak Frequencies[1]	Source
$(Al_2(H_2O)_8OH_2)^{4+}$	3520,3300,3130,2500,1950,1080,980,790,730,630	Ref 24
H_2O	3490,1650,700	Ref 24
$Al(OH)_3$	3480,1620,1010,760,530	Sadtler Index Y18K
Al_2O_3	700,450	" Y175K
1.6:1 $AlCl_3$/ImCl + H_2O	3323, 1118,703	This work
1.6:1 $AlCl_3$/ImCl + D_2O	2477(0.75),853(0.76),662(0.94)	"
0.4:1 $AlCl_3$/ImCl + H_2O	3520,3360,3100,2410,2170,2050,1170,1180	"
0.4:1 $AlCl_3$/ImCl + D_2O	2423(0.72),2265(0.73)	"

(1) Figures in brackets are the ratio of the peak frequency in H_2O to the frequency in D_2O

REFERENCES

1. Linga, H.; Stojek, Z.; Osteryoung, R. A. J. Am. Chem. Soc. 1981, 103, 3754.

2. Fanin, A. A.; King, L. A.; Levisky, J. A.; Wilkes, J. S. J. Phys. Chem., in press.

3. Taulelle, F.; Popov, A. Polyhedron 1983, 2, 889.

4. Devlin, J.; Li, P.; Cooney, R. "Molten Salts", Ed. by G. Mamantov; Dekker: New York 1969, pg. 209.

5. Bandy, A.; Devlin, J.; Burger, R.; McCoy, B. Rev. Sci. Instr. 1964, 35, 1206.

6. Grasseli, J.; Griffiths, P.; Hannah, R. in Applied Spectroscopy 1982, 36(2), 87.

7. Robinson, J.; Osteryoung, R. A. J. Am. Chem. Soc. 1979, 101, 323.

8. Wilkes, J.; Levisky, J.; Wilson, J.; Hussey, G. Inorg. Chem. 1982, 21, 1263.

9. Gale, R.; Osteryoung, R. A. Inorg. Chem. 1980, 19, 2240.

10. Vidrine, W. Anal. Chem. 1980, 52, 92.

11. Fannin, A.; King, L.; Stech, D.; Vaughn, R.; Wilkes, J.; Williams, J. "Proceedings of the Symposium on Transport Processes in Electrochemical Systems", The Electrochemical Society, Montreal, 1982, May 9-14, in press.

12. Spinner, E. Aust. J. Chem. 1967, 20, 1805.

13. Bellamy, L. "The Infrared Spectra of Complex Molecules", Chapman and Hall: London, 1975; pg. 29.

14. Sykes, P. "A Guidebook to Mechanisms in Organic Chemistry", 4th Ed., Richard Clay Ltd.: 1965, pg. 18.

15. Lord, R.; Marston, A.; Miller, F. Spectrochim. Acta 1957, 9, 113.

16. Bellocq, A.; Perchard, C.; Novak, A.; Josien, M. J. Chim. Phys. 1965, 62, 1334: Perchard, C.; Novak, A. ibid., 1968, 48, 3079.

17. Hodgson, J.; Percy, C.; Thornton, D. J. Mol. Structure 1980, 66, 81.

18. Pouchert, C. "The Aldrich Library of IR Spectra", 3rd Ed., Aldrich Chem. Co.; 1981; pg. 1195.

19. Cordes, M.; Walter, J. Spectrochim. Acta, Part A 1968, 24, 237.

20. Majoube, M. J. Mol. Structure 1980, 61, 137.

21. Leonard, N.; Gash, V. J. Am. Chem. Soc. 1954, 76, 2781.

22. Leonard, N.; Thomas, P.; Gash, V. J. Am. Chem. Soc. 1955, 77, 1552.

23. Nakamoto, K. "IR and Raman Spectra of Inorganic and Coordination Compounds", Wiley Interscience: New York, 1978.

24. Moolenaar, R.; Evans, J.; McKeever, L. J. Phys. Chem. 1970, 74, 3629.

25. McIntyre, J.; Foley, R.; Brown, B. J. Appl. Spectroscopy 1982, 36(2), 128.

26. Riesgraf, D.; May, M. J. Appl. Spectroscopy 1978, 32(4), 362.

27. Tremillon, B.; Bermond, A.; Molina, R. J. Electroanal. Chem. 1976, 74, 53.

28. Sahami, S.; Osteryoung, R. A. Anal. Chem. 1983, 55, 1970.

ACKNOWLEDGEMENT

Discussions with Mr. T. Zawodzinski, Dr's. Zenon Karpinski, Saeed Sahami, M. Lipsztajn, and John O'Dea contributed to this work as did discussions with Dr. John Wilkes of the Frank J. Seiler Laboratory of the United States Air Force Academy and with Professor C. D. Ritchie.

CREDIT

This work was supported in part by the Office of Naval Research.

FIGURE CAPTIONS

1. Configuration of IR cell.
2. IR spectrum of empty cell with parallel windows (full line) and with tilted windows (dotted line).
3. Tilted cell window configuration.
4. IR spectrum of empty cell (full line) and with 0.8:1 $AlCl_3$/BuPyCl melt (dotted line). Data unsmoothed.
5. IR spectrum of 0.8:1 (full line) and 2.0:1 (dotted line) $AlCl_3$/BuPyCl melts. Data unsmoothed.
6. IR spectrum of a) 0.8:1 and b) 1.8:1 $AlCl_3$/BuPyCl melts. Data unsmoothed.
7. IR spectrum of 0.8:1, 1.2:1 and 2:1 $AlCl_3$/BuPyCl melts. Data unsmoothed.
8. IR spectrum of 0.4:1 (dotted line) and 1.5:1 (full line) $AlCl_3$/ImCl melts. Data unsmoothed.
9. Superimposition of 1:1, 1.2:1, 1.5:1 and 1.75:1 $AlCl_3$/ImCl melts. 11 point data smoothing.
10. IR spectrum of 0.4:1, 0.55:1, 0.7:1, 0.85:1 and 0.95:1 $AlCl_3$/ImCl melts. 11 data point smooth.
11. IR spectrum of 0.4:1 (solid line) and 1.5:1 (dashed line) $AlCl_3$/ImCl melts. Data unsmoothed.
12. IR spectrum of 0.4:1, 0.70:1, 0.95:1 and 1.5:1 $AlCl_3$/ImCl melts. 11 point data smooth.

13. IR spectrum of 1.6:1 $AlCl_3$/ImCl melt after the addition of water (20 mM) and subtraction of a reference 1.6:1 $AlCl_3$/ImCl melt. 11 point data smooth.

14. IR spectrum of a 1.6:1 $AlCl_3$/ImCl melt after the addition of D_2O (60 mM) and subtraction of a reference 1.6:1 $AlCl_3$/ImCl melt. 11 point data smooth.

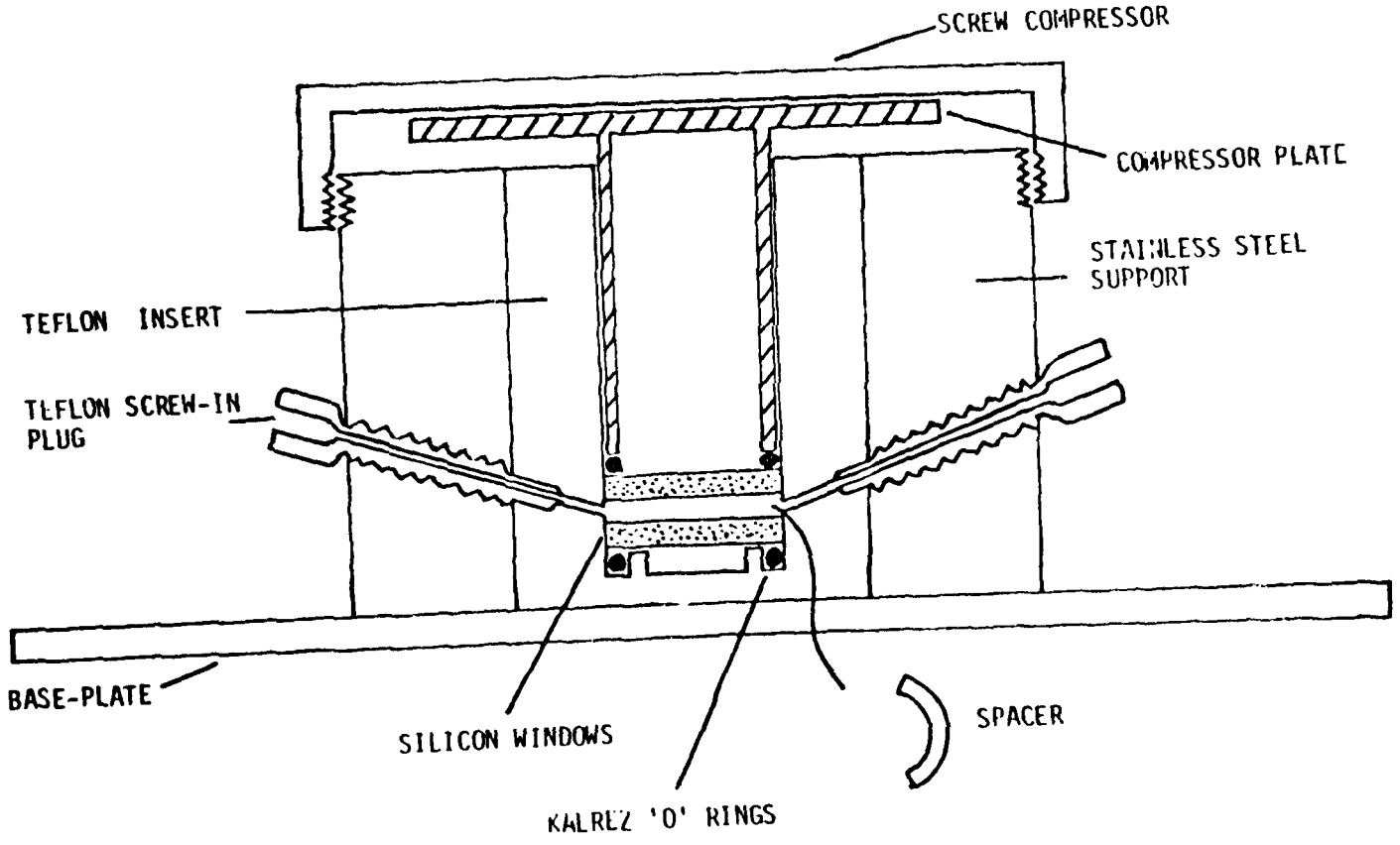
SCREW COMPRESSOR
COMPRESSOR PLATE
STAINLESS STEEL SUPPORT
TEFLON INSERT
TEFLON SCREW-IN PLUG
BASE-PLATE
SILICON WINDOWS
KALREZ 'O' RINGS
SPACER

Figure 1

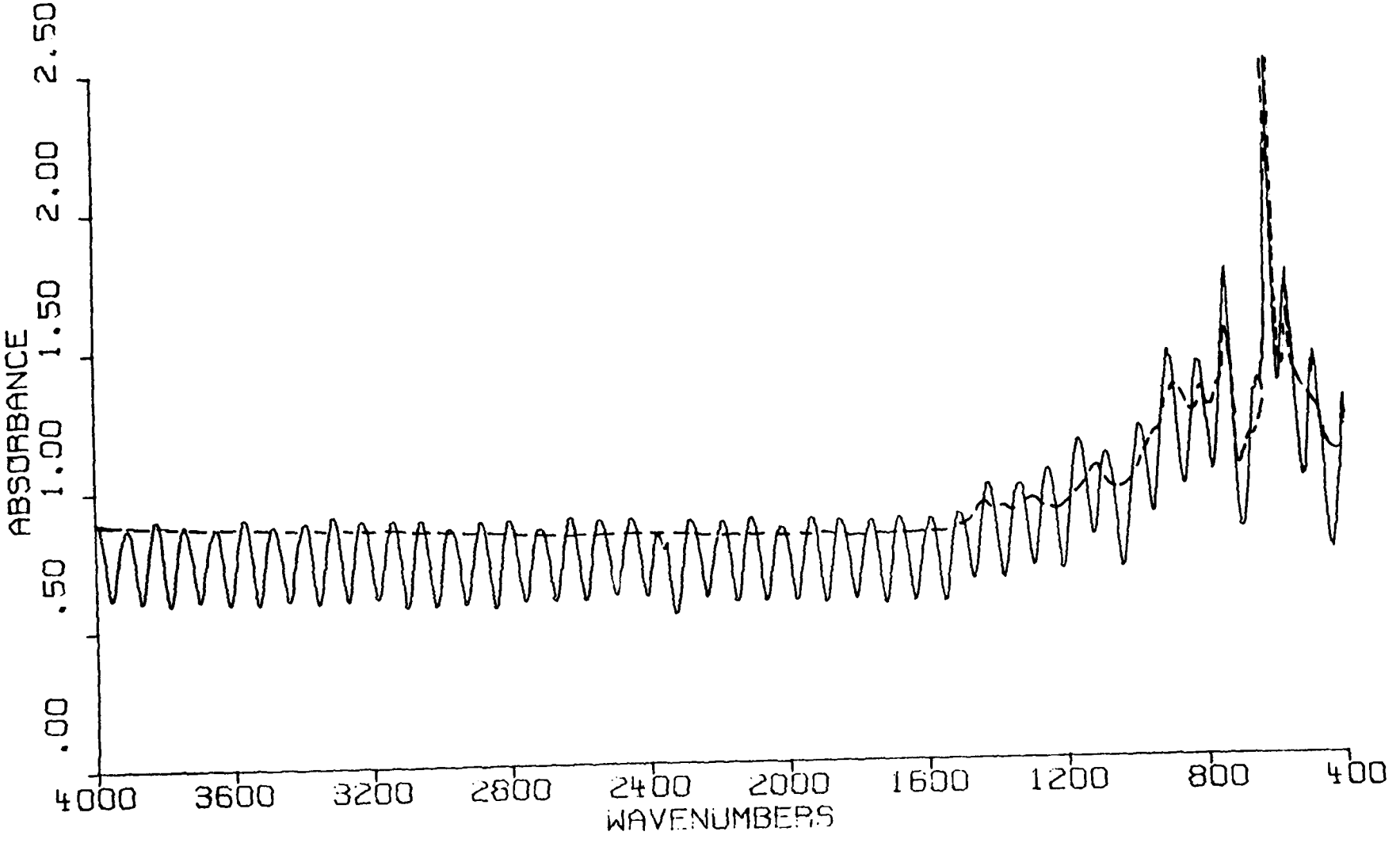
ABSORBANCE
.00
.50
1.00
1.50
2.00
2.50
4000
3600
3200
2800
2400
2000
1600
1200
800
400
WAVENUMBERS

Figure 2

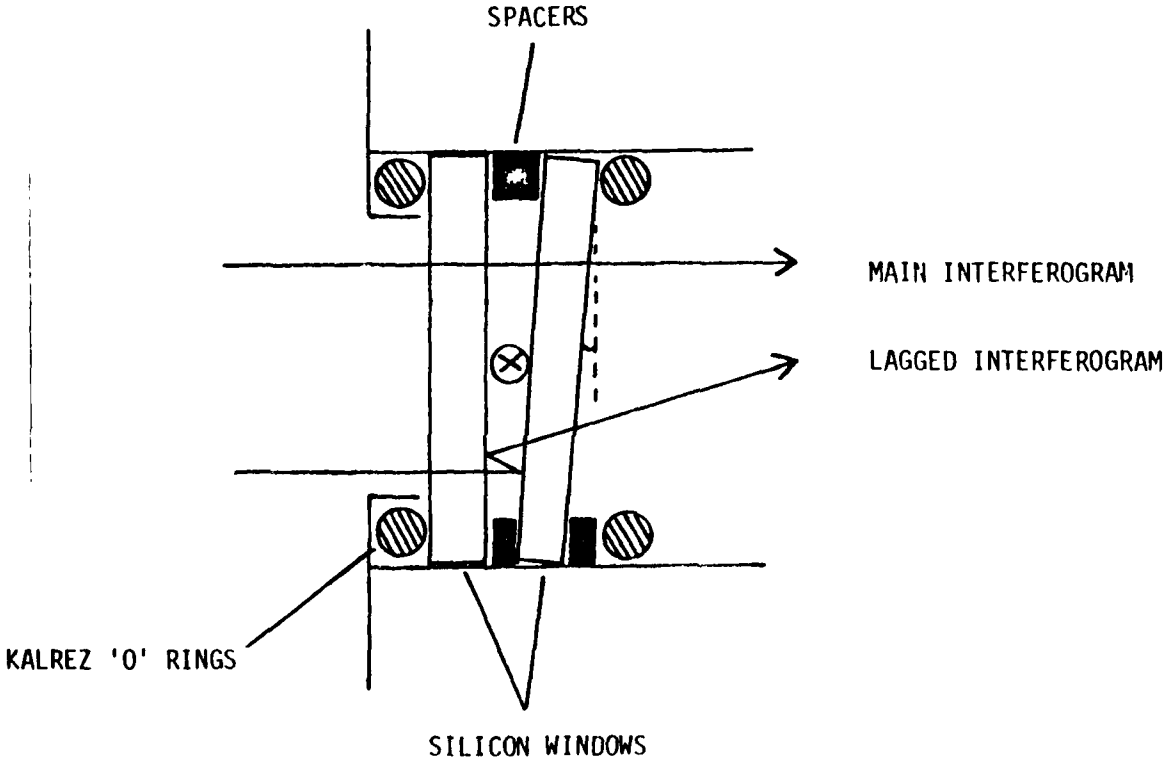
SPACERS
MAIN INTERFEROGRAM
LAGGED INTERFEROGRAM
KALREZ 'O' RINGS
SILICON WINDOWS

Figure 3

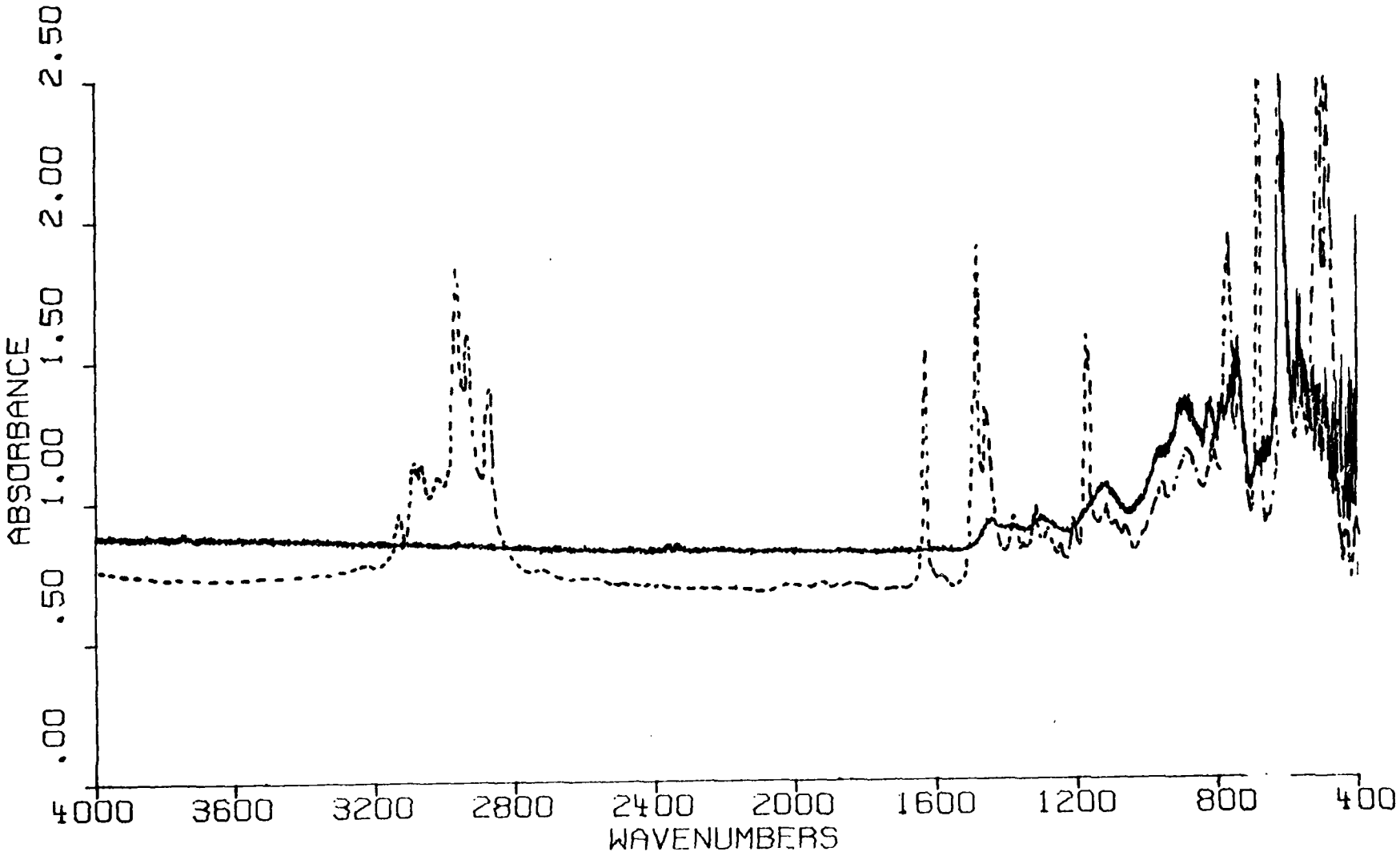
ABSORBANCE
.00
.50
1.00
1.50
2.00
2.50
4000
3600
3200
2800
2400
2000
1600
1200
800
400
WAVENUMBERS

Figure 4

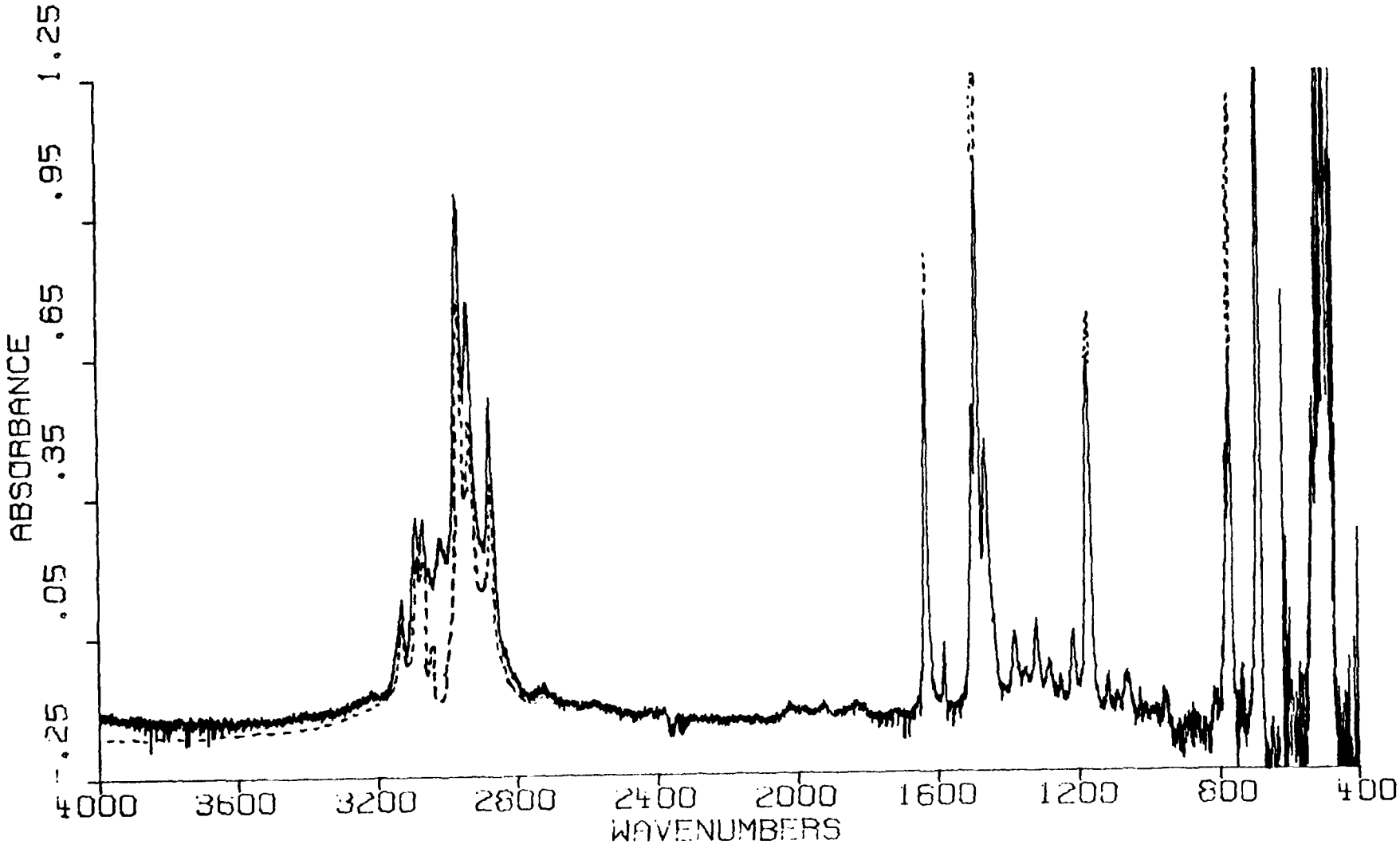
ABSORBANCE
1.25
.95
.65
.35
.05
-.25
4000
3600
3200
2800
2400
2000
1600
1200
800
400
WAVENUMBERS

Figure 5

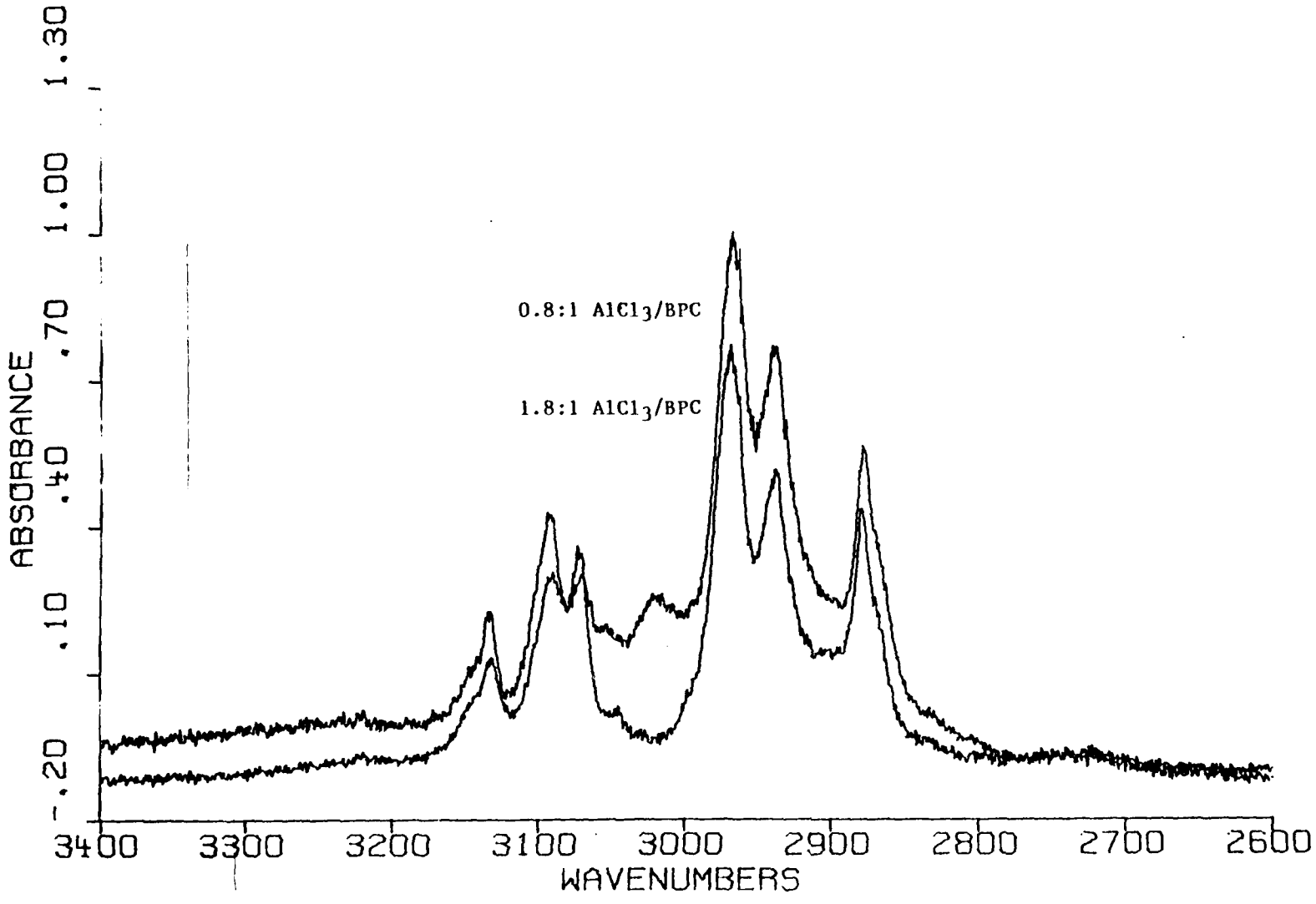
ABSORBANCE
1.30
1.00
.70
.40
.10
-.20
0.8:1 AlCl3/BPC
1.8:1 AlCl3/BPC
3400
3300
3200
3100
3000
2900
2800
2700
2600
WAVENUMBERS

Figure 6

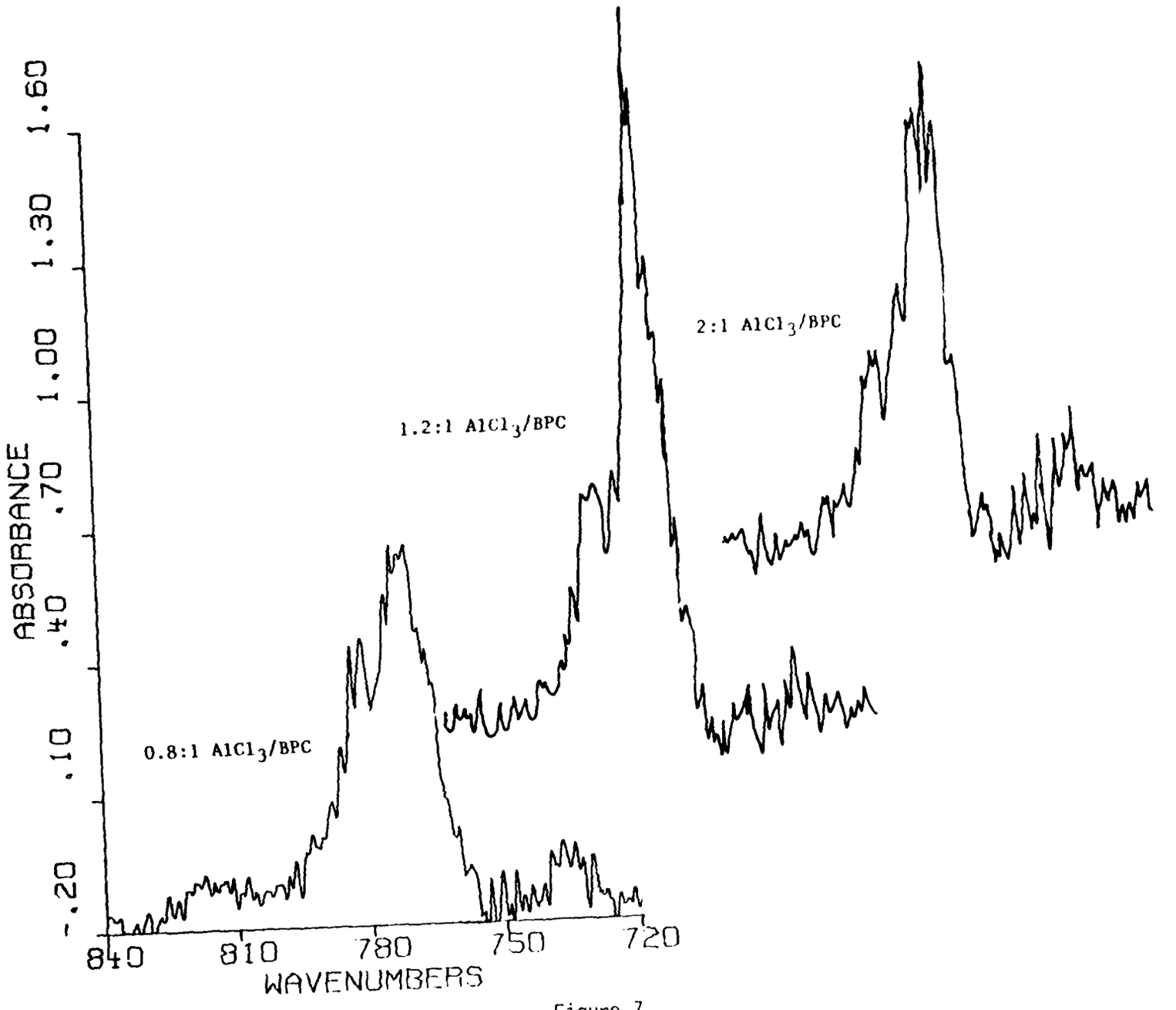
ABSORBANCE
1.60
1.30
1.00
.70
.40
.10
-.20
0.8:1 AlCl3/BPC
1.2:1 AlCl3/BPC
2:1 AlCl3/BPC
840
810
780
750
720
WAVENUMBERS

Figure 7

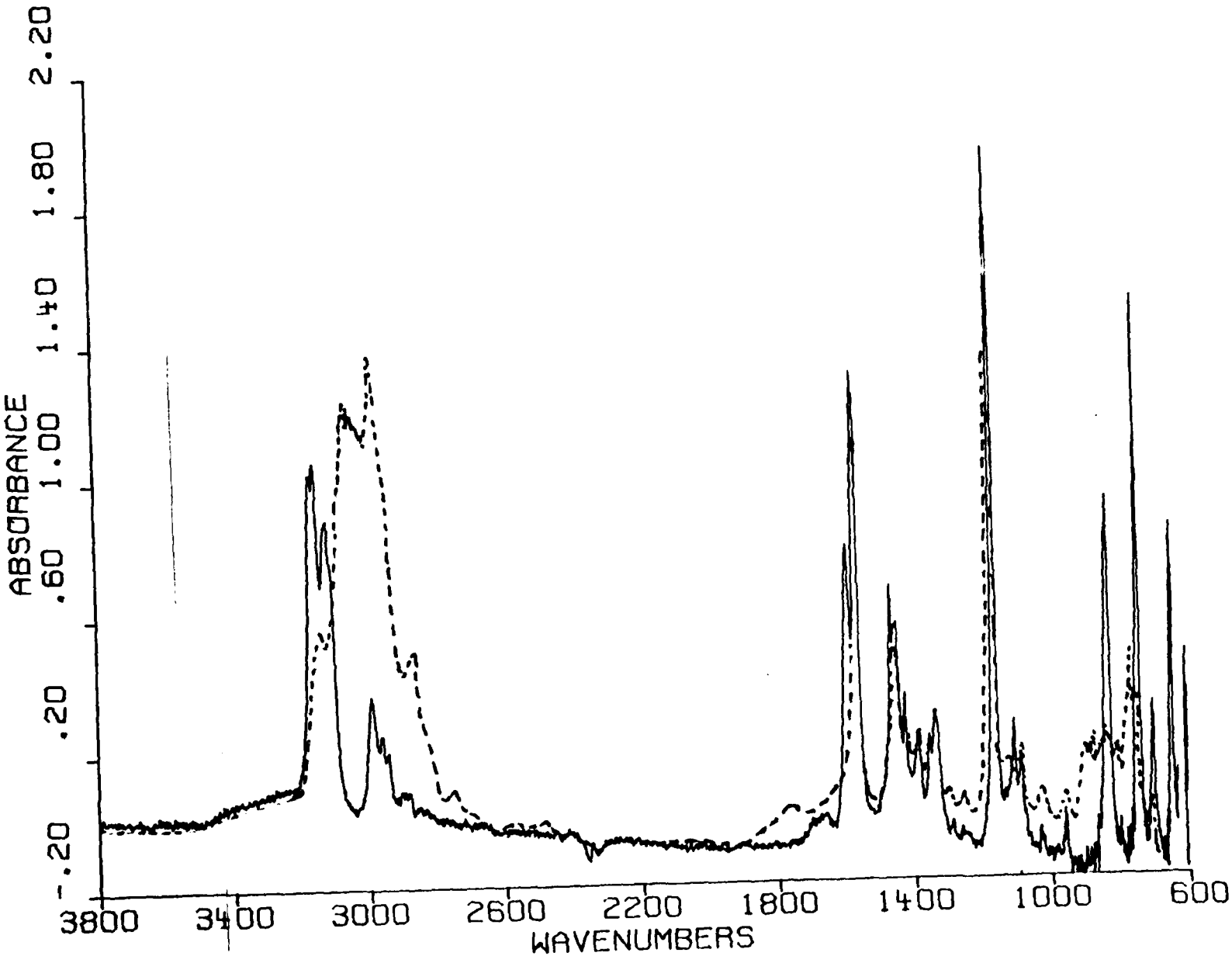
ABSORBANCE
2.20
1.80
1.40
1.00
.60
.20
-.20
3800
3400
3000
2600
2200
1800
1400
1000
600
WAVENUMBERS

Figure 8

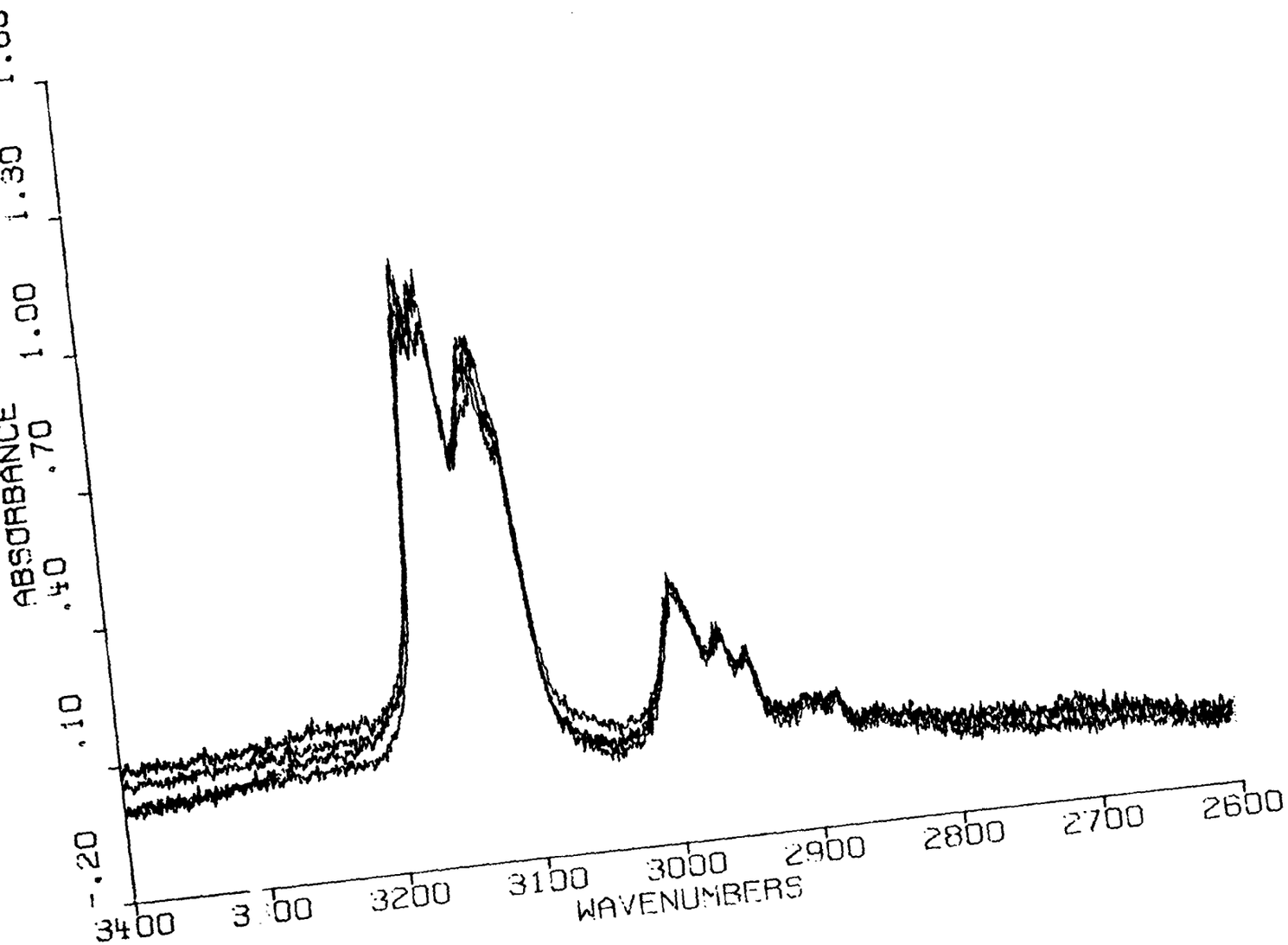
ABSORBANCE
1.60
1.30
1.00
.70
.40
.10
-.20
3400
3300
3200
3100
3000
2900
2800
2700
2600
WAVENUMBERS

Figure 9

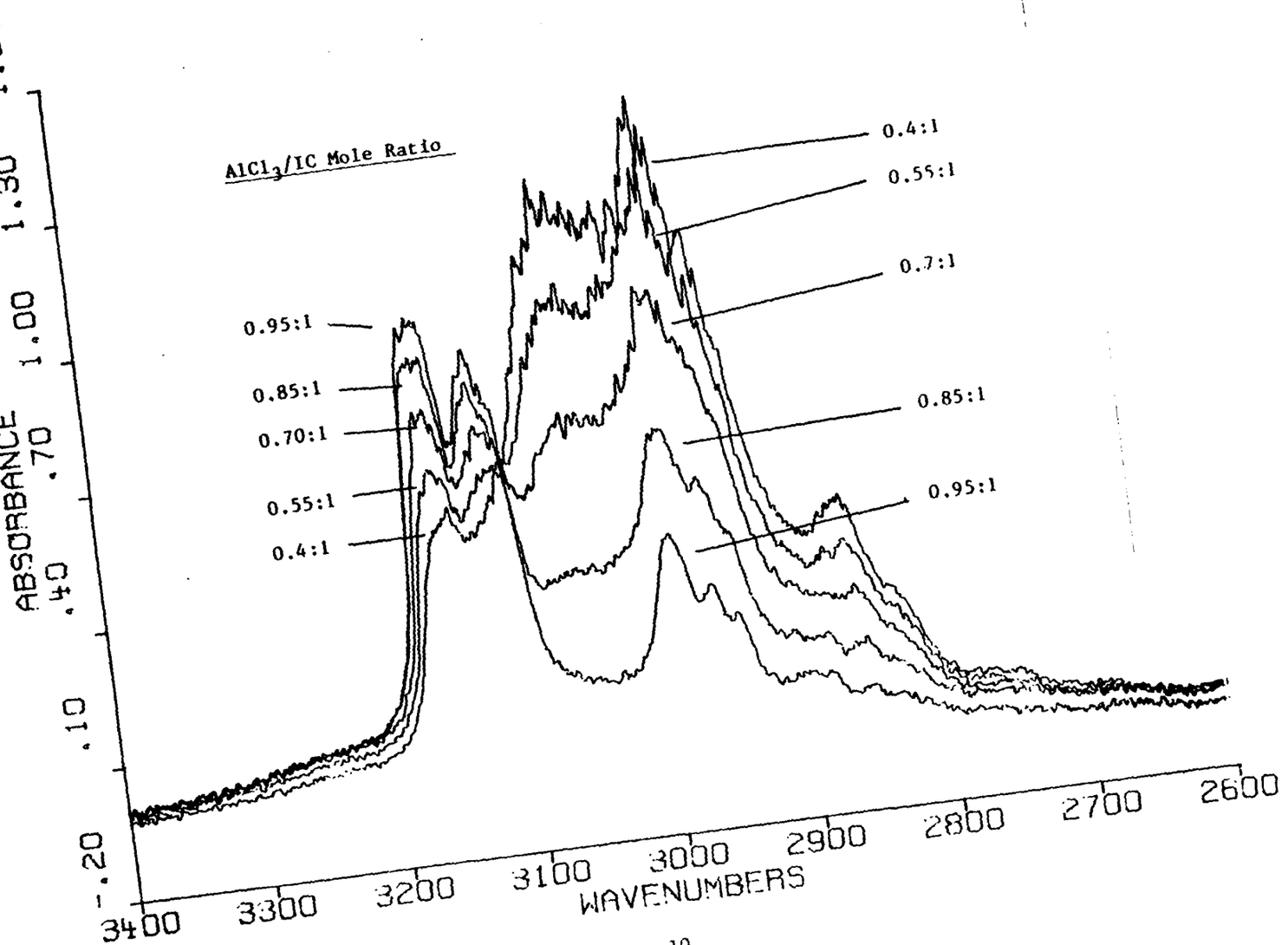
AlCl3/IC Mole Ratio
0.4:1
0.55:1
0.7:1
0.85:1
0.95:1
0.95:1
0.85:1
0.70:1
0.55:1
0.4:1
ABSORBANCE
1.60
1.30
1.00
.70
.40
.10
-.20
3400
3300
3200
3100
3000
2900
2800
2700
2600
WAVENUMBERS

Figure 10

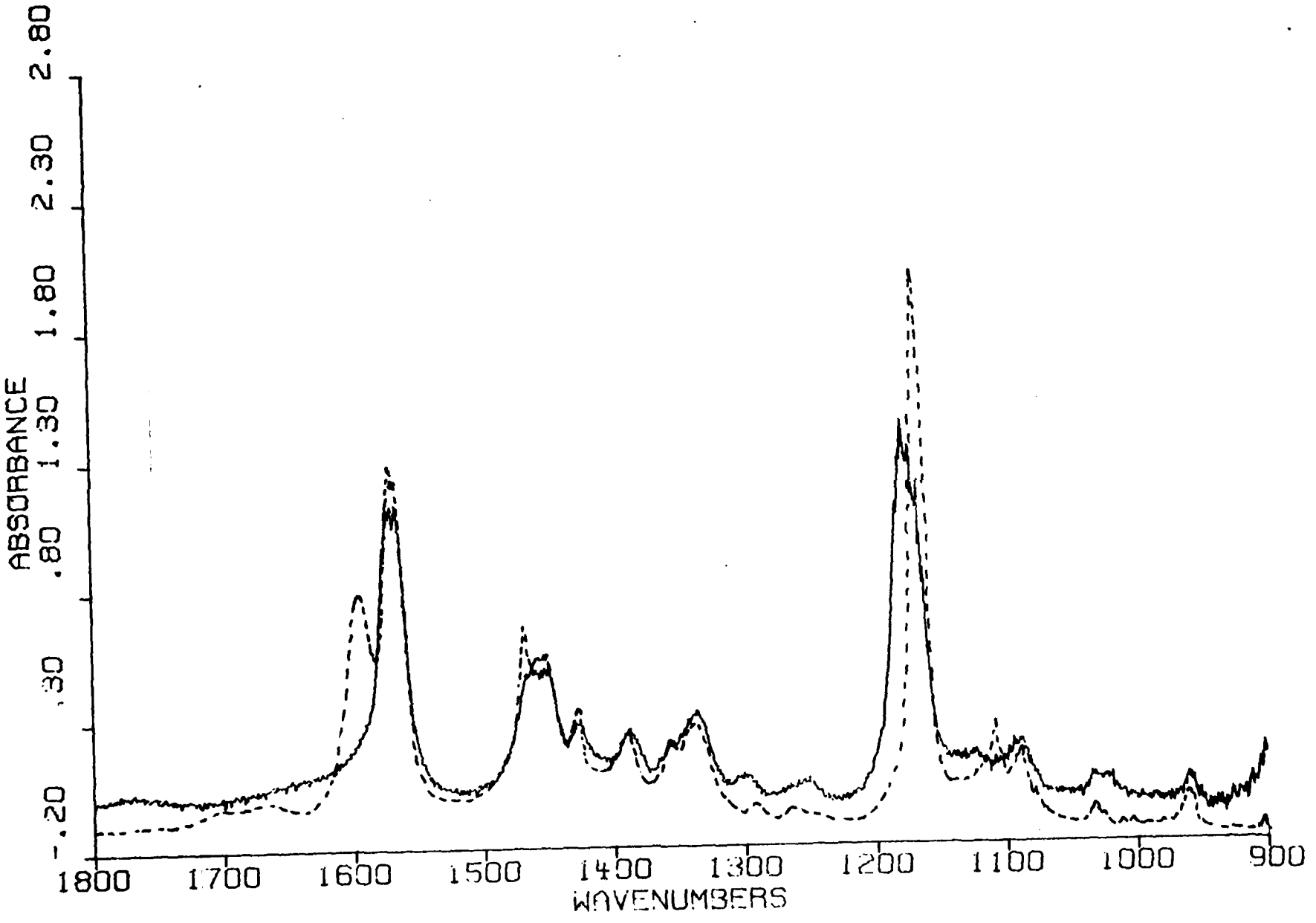
ABSORBANCE
2.80
2.30
1.80
1.30
.80
.30
-.20
1800
1700
1600
1500
1400
1300
1200
1100
1000
900
WAVENUMBERS

Figure 11

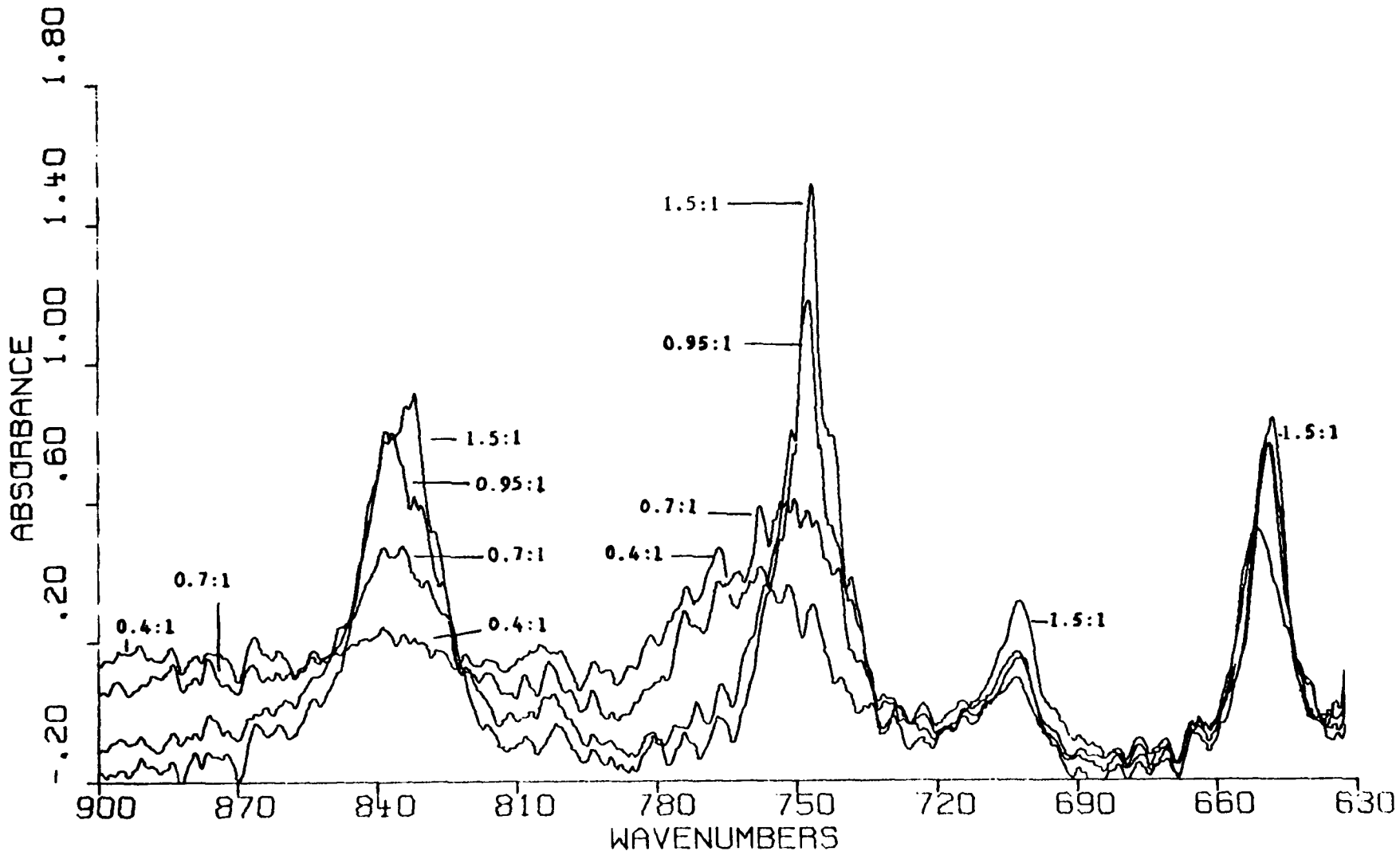
ABSORBANCE
1.80
1.40
1.00
.60
.20
-.20
900
870
840
810
780
750
720
690
660
630
WAVENUMBERS
1.5:1
0.95:1
0.7:1
0.4:1
1.5:1
0.95:1
0.7:1
0.4:1
0.7:1
0.4:1
1.5:1
1.5:1

Figure 12

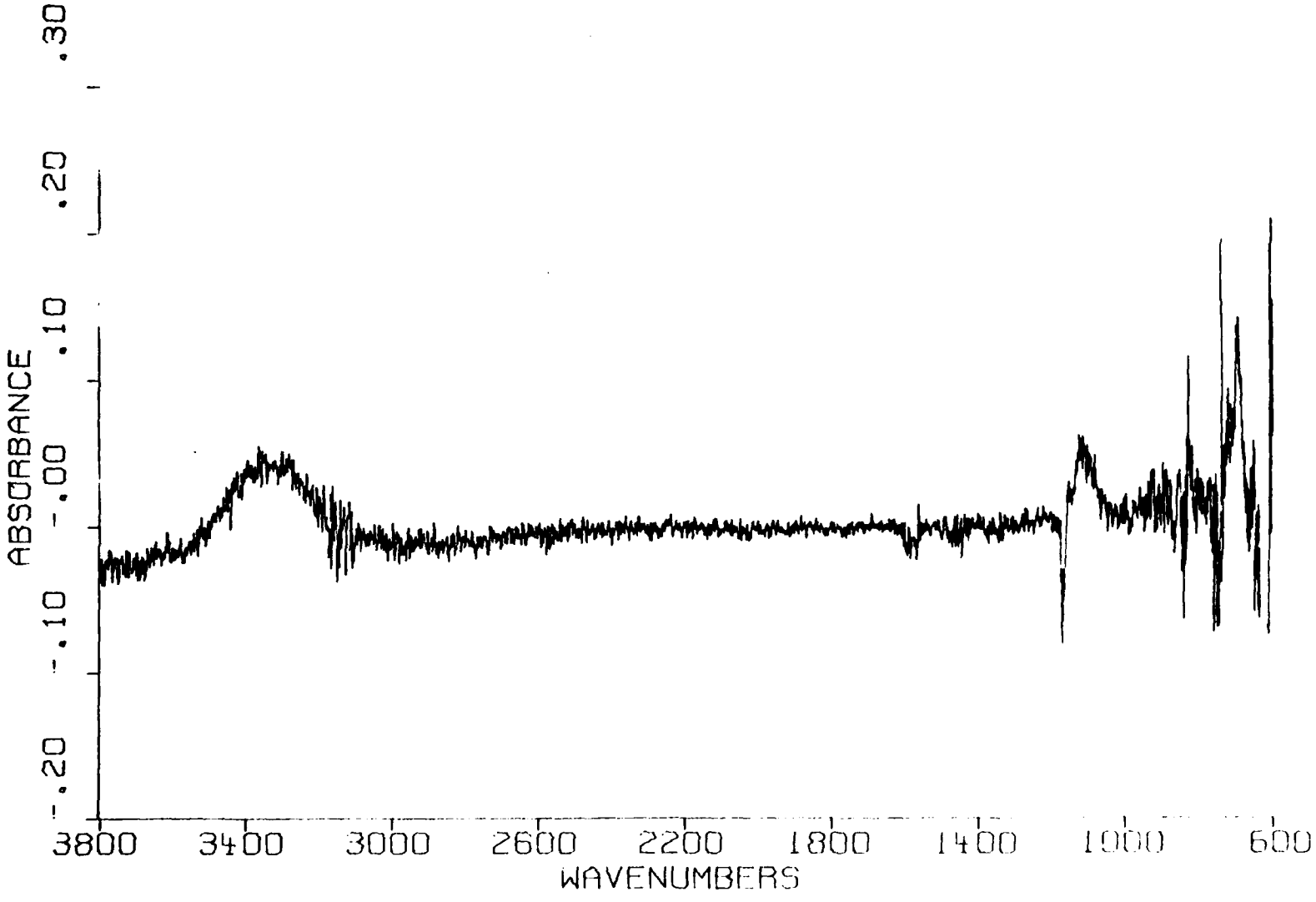
ABSORBANCE
.30
.20
.10
-.00
-.10
-.20
3800
3400
3000
2600
2200
1800
1400
1000
600
WAVENUMBERS

Figure 13

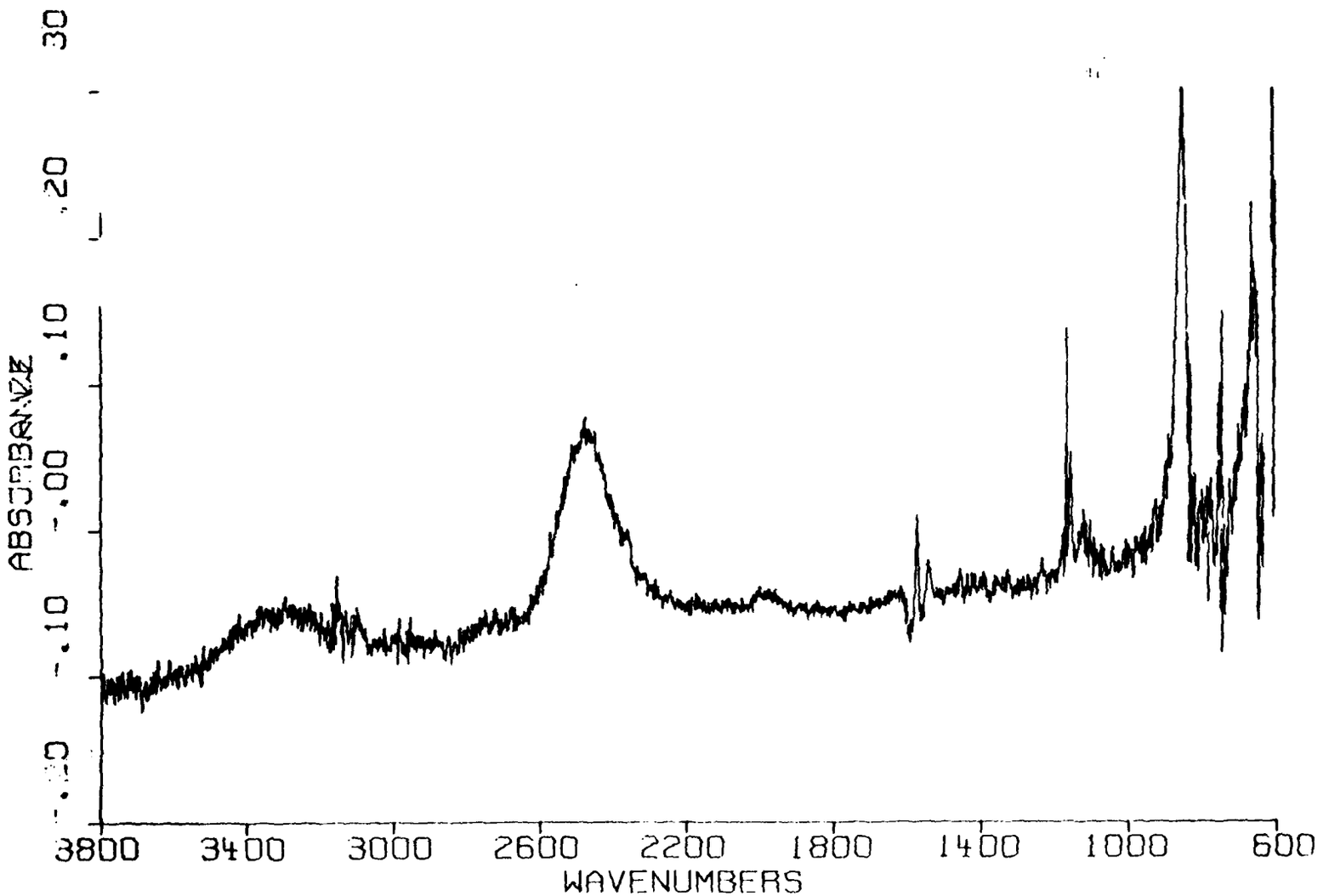
30
.20
.10
-.00
-.10
3800
3400
3000
2600
2200
1800
1400
1000
600
WAVENUMBERS

Figure 14

DL/413/83/01
GEN/413-2

TECHNICAL REPORT DISTRIBUTION LIST, GEN

	No. Copies
Office of Naval Research Attn: Code 413 800 N. Quincy Street Arlington, Virginia 22217	2
ONR Pasadena Detachment Attn: Dr. R. J. Marcus 1030 East Green Street Pasadena, California 91106	1
Commander, Naval Air Systems Command Attn: Code 310C (H. Rosenwasser) Washington, D.C. 20360	1
Naval Civil Engineering Laboratory Attn: Dr. R. W. Drisko Port Hueneme, California 93401	1
Superintendent Chemistry Division, Code 6100 Naval Research Laboratory Washington, D.C. 20375	1
Defense Technical Information Center Building 5, Cameron Station Alexandria, Virginia 22314	12
DTNSRDC Attn: Dr. G. Bosmajian Applied Chemistry Division Annapolis, Maryland 21401	1
Naval Ocean Systems Center Attn: Dr. S. Yamamoto Marine Sciences Division San Diego, California 91232	1
Naval Ocean Systems Center Attn: Technical Library San Diego, California 92152	1
Naval Weapons Center Attn: Dr. A. B. Amster Chemistry Division China Lake, California 93555	1
Scientific Advisor Commandant of the Marine Corps Code RD-1 Washington, D.C. 20380	1
Dean William Tolles Naval Postgraduate School Monterey, California 93940	1
U.S. Army Research Office Attn: CRD-AA-IP P.O. Box 12211 Research Triangle Park, NC 27709	1
Mr. Vincent Schaper DTNSRDC Code 2830 Annapolis, Maryland 21402	1
Mr. John Boyle Materials Branch Naval Ship Engineering Center Philadelphia, Pennsylvania 19112	1
Mr. A. M. Anzalone Administrative Librarian PLASTEC/ARRADCOM Bldg 3401 Dover, New Jersey 07801	1

DL/413/83/01
051B/413-2

TECHNICAL REPORT DISTRIBUTION LIST, 051B

Dr. M. B. Denton
Department of Chemistry
University of Arizona
Tucson, Arizona 85721

Dr. R. A. Osteryoung
Department of Chemistry
State University of New York
Buffalo, New York 14214

Dr. J. Osteryoung
Department of Chemistry
State University of New York
Buffalo, New York 14214

Dr. B. R. Kowalski
Department of Chemistry
University of Washington
Seattle, Washington 98105

Dr. H. Freiser
Department of Chemistry
University of Arizona
Tucson, Arizona 85721

Dr. H. Chernoff
Department of Mathematics
Massachusetts Institute of Technology
Cambridge, Massachusetts 02139

Dr. A. Zirino
Naval Undersea Center
San Diego, California 92132

Professor George H. Morrison
Department of Chemistry
Cornell University
Ithaca, New York 14853

Dr. Alan Bewick
Department of Chemistry
Southampton University
Southampton, Hampshire
ENGLAND 5095NA

Dr. S. P. Perone
Lawrence Livermore Laboratory L-370
P.O. Box 808
Livermore, California 94550

Dr. L. Jarvis
Code 6100
Naval Research Laboratory
Washington, D.C. 20375

Dr. G. M. Hieftje
Department of Chemistry
Indiana University
Bloomington, Indiana 47401

Dr. Christie G. Enke
Department of Chemistry
Michigan State University
East Lansing, Michigan 48824

Dr. D. L. Venezky
Naval Research Laboratory
Code 6130
Washington, D.C. 20375

Walter G. Cox, Code 3632
Naval Underwater Systems Center
Building 148
Newport, Rhode Island 02840

Professor Isiah M. Warner
Department of Chemistry
Emory University
Atlanta, Georgia 30322

Dr. Kent Eisentraut
Air Force Materials Laboratory
Wright-Patterson AFB, Ohio 45433

Dr. Adolph B. Amster
Chemistry Division
Naval Weapons Center
China Lake, California 93555

Dr. B. E. Douda
Chemical Sciences Branch
Code 50 C
Naval Weapons Support Center
Crane, Indiana 47322

Dr. John Eyler
Department of Chemistry
University of Florida
Gainesville, Florida 32611

DL/413/83/01
051B/413-2

TECHNICAL REPORT DISTRIBUTION LIST, 051B

Professor J. Janata
Department of Bioengineering
University of Utah
Salt Lake City, Utah 84112

Dr. J. DeCorpo
NAVSEA
Code 05R14
Washington, D.C. 20362

Dr. Charles Anderson
Analytical Chemistry Division
Athens Environmental Laboratory
College Station Road
Athens, Georgia 30613

Dr. Ron Flemming
B 108 Reactor
National Bureau of Standards
Washington, D.C. 20234

Dr. David M. Hercules
Department of Chemistry
University of Pittsburgh
Pittsburgh, Pennsylvania

Dr. Frank Herr
Office of Naval Research
Code 422CB
800 N. Quincy Street
Arlington, Virginia 22217

Professor E. Keating
Department of Mechanical Engineering
U.S. Naval Academy
Annapolis, Maryland 21401

Dr. M. H. Miller
1133 Hampton Road
Route 4
U.S. Naval Academy
Annapolis, Maryland 21401

Dr. Clifford Spiegelman
National Bureau of Standards
Room A337 Bldg. 101
Washington, D.C. 20234

Dr. Denton Elliott
AFOSR/NC
Bolling AFB
Washington, D.C. 20362

Dr. B. E. Spielvogel
Inorganic and Analytical Branch
P.O. Box 12211
Research Triangle Park, NC 27709

Ms. Ann De Witt
Material Science Department
160 Fieldcrest Avenue
Raritan Center
Edison, New Jersey 08818

Dr. A. Harvey
Code 6110
Naval Research Laboratory
Washington, D.C. 20375

Dr. John Hoffsommer
Naval Surface Weapons Center
Building 30 Room 208
Silver Spring, Maryland 20910

Mr. S. M. Hurley
Naval Facilities Engineering Command
Code 032P
200 Stovall Street
Alexandria, Virginia 22331

Ms. W. Parkhurst
Naval Surface Weapons Center
Code R33
Silver Spring, Maryland 20910

Dr. M. Robertson
Electrochemical Power Sources Division
Code 305
Naval Weapons Support Center
Crane, Indiana 47522

CDR Andrew T. Zander
10 Country Club Lane
ONR Boston
Plaistow, New Hampshire 03865

DL/413/83/01
051B/413-2

TECHNICAL REPORT DISTRIBUTION LIST, 051B

Dr. Robert W. Shaw
U.S. Army Research Office
Box 12211
Research Triangle Park, NC 27709

Dr. Marvin Wilkerson
Naval Weapons Support Center
Code 30511
Crane, Indiana 47522

Dr. J. Wyatt
Naval Research Laboratory
Code 6110
Washington, D.C. 20375

Dean William Tolles
Naval Post Graduate School
Spanaugel Hall
Monterey, California 93940

Dr. H. Wohltjen
Naval Research Laboratory
Code 6170
Washington, D.C. 20375

DL/413/83/01
359/413-2

TECHNICAL REPORT DISTRIBUTION LIST, 359

Dr. Paul Delahay
Department of Chemistry
New York University
New York, New York 10003

Dr. P. J. Hendra
Department of Chemistry
University of Southampton
Southampton S09 5NH
United Kingdom

Dr. T. Katan
Lockheed Missiles and
Space Co., Inc.
P.O. Box 504
Sunnyvale, California 94088

Dr. D. N. Bennion
Department of Chemical Engineering
Brighma Young University
Provo, Utah 84602

Dr. R. A. Marcus
Department of Chemistry
California Institute of Technology
Pasadena, California 91125

Mr. Joseph McCartney
Code 7121
Naval Ocean Systems Center
San Diego, California 92152

Dr. J. J. Auborn
Bell Laboratories
Murray Hill, New Jersey 07974

Dr. Joseph Singer, Code 302-1
NASA-Lewis
21000 Brookpark Road
Cleveland, Ohio 44135

Dr. P. P. Schmidt
Department of Chemistry
Oakland University
Rochester, Michigan 48063

Dr. H. Richtol
Chemistry Department
Rensselaer Polytechnic Institute
Troy, New York 12181

Dr. E. Yeager
Department of Chemistry
Case Western Reserve University
Cleveland, Ohio 44106

Dr. C. E. Mueller
The Electrochemistry Branch
Naval Surface Weapons Center
White Oak Laboratory
Silver Spring, Maryland 20910

Dr. Sam Perone
Chemistry & Materials
Science Department
Lawrence Livermore National Lab.
Livermore, California 94550

Dr. Royce W. Murray
Department of Chemistry
University of North Carolina
Chapel Hill, North Carolina 27514

Dr. G. Goodman
Johnson Controls
5757 North Green Bay Avenue
Milwaukee, Wisconsin 53201

Dr. B. Brummer
EIC Incorporated
111 Chapel Street
Newton, Massachusetts 02158

Dr. Adam Heller
Bell Laboratories
Murray Hill, New Jersey 07974

Electrochimica Corporation
Attn: Technical Library
2485 Charleston Road
Mountain View, California 94040

Library
Duracell, Inc.
Burlington, Massachusetts 01803

Dr. A. B. Ellis
Chemistry Department
University of Wisconsin
Madison, Wisconsin 53706

DL/413/83/01
359/413-2

TECHNICAL REPORT DISTRIBUTION LIST, 359

Dr. M. Wrighton
Chemistry Department
Massachusetts Institute
of Technology
Cambridge, Massachusetts 02139

Dr. B. Stanley Pons
Department of Chemistry
University of Utah
Salt Lake City, Utah 84112

Donald E. Mains
Naval Weapons Support Center
Electrochemical Power Sources Division
Crane, Indiana 47522

S. Ruby
DOE (STOR)
M.S. 6B025 Forrestal Bldg.
Washington, D.C. 20595

Dr. A. J. Bard
Department of Chemistry
University of Texas
Austin, Texas 78712

Dr. Janet Osteryoung
Department of Chemistry
State University of New York
Buffalo, New York 14214

Dr. Donald W. Ernst
Naval Surface Weapons Center
Code R-33
White Oak Laboratory
Silver Spring, Maryland 20910

Mr. James R. Moden
Naval Underwater Systems Center
Code 3632
Newport, Rhode Island 02840

Dr. Bernard Spielvogel
U.S. Army Research Office
P.O. Box 12211
Research Triangle Park, NC 27709

Dr. William Ayers
ECD Inc.
P.O. Box 5357
North Branch, New Jersey 08876

Dr. M. M. Nicholson
Electronics Research Center
Rockwell International
3370 Miraloma Avenue
Anaheim, California

Dr. Michael J. Weaver
Department of Chemistry
Purdue University
West Lafayette, Indiana 47907

Dr. R. David Rauh
EIC Corporation
111 Chapel Street
Newton, Massachusetts 02158

Dr. Aaron Wold
Department of Chemistry
Brown University
Providence, Rhode Island 02192

Dr. Martin Fleischmann
Department of Chemistry
University of Southampton
Southampton SO9 5NH ENGLAND

Dr. R. A. Osteryoung
Department of Chemistry
State University of New York
Buffalo, New York 14214

Dr. Denton Elliott
Air Force Office of Scientific
Research
Bolling AFB
Washington, D.C. 20332

Dr. R. Nowak
Naval Research Laboratory
Code 6130
Washington, D.C. 20375

Dr. D. F. Shriver
Department of Chemistry
Northwestern University
Evanston, Illinois 60201

Dr. Aaron Fletcher
Naval Weapons Center
Code 3852
China Lake, California 93555

DL/413/83/01
359/413-2

TECHNICAL REPORT DISTRIBUTION LIST, 359

Dr. David Aikens
Chemistry Department
Rensselaer Polytechnic Institute
Troy, New York 12181

Dr. A. P. B. Lever
Chemistry Department
York University
Downsview, Ontario M3J1P3

Dr. Stanislaw Szpak
Naval Ocean Systems Center
Code 6343, Bayside
San Diego, California 95152

Dr. Gregory Farrington
Department of Materials Science
and Engineering
University of Pennsylvania
Philadelphia, Pennsylvania 19104

M. L. Robertson
Manager, Electrochemical
and Power Sources Division
Naval Weapons Support Center
Crane, Indiana 47522

Dr. T. Marks
Department of Chemistry
Northwestern University
Evanston, Illinois 60201

Dr. Micha Tomkiewicz
Department of Physics
Brooklyn College
Brooklyn, New York 11210

Dr. Lesser Blum
Department of Physics
University of Puerto Rico
Rio Piedras, Puerto Rico 00931

Dr. Joseph Gordon, II
IBM Corporation
K33/281
5600 Cottle Road
San Jose, California 95193

Dr. D. H. Whitmore
Department of Materials Science
Northwestern University
Evanston, Illinois 60201

Dr. Alan Bewick
Department of Chemistry
The University of Southampton
Southampton, S09 5NH ENGLAND

Dr. E. Anderson
NAVSEA-56Z33 NC #4
2541 Jefferson Davis Highway
Arlington, Virginia 20362

Dr. Bruce Dunn
Department of Engineering &
Applied Science
University of California
Los Angeles, California 90024

Dr. Elton Cairns
Energy & Environment Division
Lawrence Berkeley Laboratory
University of California
Berkeley, California 94720

Dr. D. Cipris
Allied Corporation
P.O. Box 3000R
Morristown, New Jersey 07960

Dr. M. Philpott
IBM Corporation
5600 Cottle Road
San Jose, California 95193

Dr. Donald Sandstrom
Department of Physics
Washington State University
Pullman, Washington 99164

Dr. Carl Kannewurf
Department of Electrical Engineering
and Computer Science
Northwestern University
Evanston, Illinois 60201

DL/413/83/01
359/413-2

TECHNICAL REPORT DISTRIBUTION LIST, 359

Dr. Robert Somoano
Jet Propulsion Laboratory
California Institute of Technology
Pasadena, California 91103

Dr. Johann A. Joebstl
USA Mobility Equipment R&D Command
DRDME-EC
Fort Belvoir, Virginia 22060

Dr. Judith H. Ambrus
NASA Headquarters
M.S. RTS-6
Washington, D.C. 20546

Dr. Albert R. Landgrebe
U.S. Department of Energy
M.S. 6B025 Forrestal Building
Washington, D.C. 20595

Dr. J. J. Brophy
Department of Physics
University of Utah
Salt Lake City, Utah 84112

Dr. Charles Martin
Department of Chemistry
Texas A&M University
College Station, Texas 77843

Dr. H. Tachikawa
Department of Chemistry
Jackson State University
Jackson, Mississippi 39217

Dr. Theodore Beck
Electrochemical Technology Corp.
3935 Leary Way N.W.
Seattle, Washington 98107

Dr. Farrell Lytle
Boeing Engineering and
Construction Engineers
P.O. Box 3707
Seattle, Washington 98124

Dr. Robert Gotscholl
U.S. Department of Energy
MS G-226
Washington, D.C. 20545

Dr. Edward Fletcher
Department of Mechanical Engineering
University of Minnesota
Minneapolis, Minnesota 55455

Dr. John Fontanella
Department of Physics
U.S. Naval Academy
Annapolis, Maryland 21402

Dr. Martha Greenblatt
Department of Chemistry
Rutgers University
New Brunswick, New Jersey 08903

Dr. John Wasson
Syntheco, Inc.
Rte 6 - Industrial Pike Road
Gastonia, North Carolina 28052

Dr. Walter Roth
Department of Physics
State University of New York
Albany, New York 12222

Dr. Anthony Sammells
Eltron Research Inc.
710 E. Ogden Avenue #108
Naperville, Illinois 60540

Dr. W. M. Risen
Department of Chemistry
Brown University
Providence, Rhode Island 02192

Dr. C. A. Angell
Department of Chemistry
Purdue University
West Lafayette, Indiana 47907

Dr. Thomas Davis
Polymer Science and Standards
Division
National Bureau of Standards
Washington, D.C. 20234


DATE
ILME